
Robust off-policy Reinforcement Learning via Soft Constrained Adversary

Kosuke Nakanishi^{*†}Akihiro Kubo^{*}Yuji Yasui[†]Shin Ishii^{*}

Abstract

Recently, robust reinforcement learning (RL) methods against input observation have garnered significant attention and undergone rapid evolution due to RL's potential vulnerability. Although these advanced methods have achieved reasonable success, there have been two limitations when considering adversary in terms of long-term horizons. First, the mutual dependency between the policy and its corresponding optimal adversary limits the development of off-policy RL algorithms; although obtaining optimal adversary should depend on the current policy, this has restricted applications to off-policy RL. Second, these methods generally assume perturbations based only on the L_p -norm, even when prior knowledge of the perturbation distribution in the environment is available. We here introduce another perspective on adversarial RL: an f-divergence constrained problem with the prior knowledge distribution. From this, we derive two typical attacks and their corresponding robust learning frameworks. The evaluation of robustness is conducted and the results demonstrate that our proposed methods achieve excellent performance in sample-efficient off-policy RL.

1 Introduction

In recent years, advancements in computational technology, coupled with the practical successes of deep neural networks (DNNs) [Krizhevsky et al., 2012, Simonyan and Zisserman, 2014, He et al., 2016], have fueled expectations for automated decision-making and control in increasingly complex environments [Kober et al., 2013, Levine et al., 2016, Kiran et al., 2021]. Deep reinforcement learning (DRL) is a promising framework for such applications, demonstrating performance that surpasses human capabilities by acquiring high-dimensional representational power through function approximation [Mnih et al., 2015, Silver et al., 2017]. However, in real-world applications, significant performance degradation in control due to adverse perturbations raises practical concerns [Huang et al., 2017, Lin et al., 2017]. Therefore, the development and testing of algorithms that consider such challenges are crucial.

Recent research [Zhang et al., 2021, Sun et al., 2021, Liang et al., 2022] identifies there are two types of vulnerabilities in DRL. The first is related to the smoothness of the policy function, which primarily arises from the function approximation properties of DNNs. The second vulnerability stems from the dynamics of the environment and is considered within the framework of Markov Decision Processes (MDPs). To understand the latter case, imagine a situation where you are going to cross over a deep valley and there are two bridges. The one is short length but a narrow bridge and the other is a large bridge but has a little bit longer path. If you have clear vision, you may prefer the former, but if you get noisy vision in foggy conditions, the latter path is the best choice to achieve your goals without the risk of falling. To realize such comprehensive decision makings, we need to consider long-term reward appropriately into adversaries and robustness for an RL problem, rather than the temporal DNN smoothness or consistency of output as in the supervised learning.

^{*}Kyoto University

[†]Honda R&D Corp.

Zhang et al. [2021], Sun et al. [2021] theoretically prove that optimal (worst-case) adversaries for a policy, capable of estimating long-term horizons, can be learned as an RL agent. Zhang et al. [2021] propose an approach where the (victim) policy and the corresponding (optimal) adversary are trained alternately, resulting in a robust agent. They refer to this framework as *Alternating Training with Learned Adversaries* (ATLA). Sun et al. [2021] extend this framework to high-dimensional state spaces and strong attacks by dividing the optimal adversary into two parts: searching for a perturbing direction in policy space (Director) and crafting a perturbation in the state space through numerical calculation (Actor), referring as *Policy Adversarial Actor Director* (PA-AD).

These methods establish robust RL frameworks on state observations with a solid foundation; however, two main issues remain unresolved. The first issue lies in the algorithms for continuous action spaces, which rely on on-policy Actor-Critic algorithms, making them unable to be applied to recently developed off-policy algorithms with good sample-efficiency and performance. To learn optimal adversary, Zhang et al. [2021], Sun et al. [2021] use the policy’s trajectories under the corresponding optimal adversary, but during training phase, RL’s policy is updated constantly, resulting in the fact the gathered trajectories cannot be used for the adversary training. The second point is that these robust learning methods assume perturbations under the constraint of L_p -norm ball in the worst-case scenario, making it difficult to consider phenomena such as Gaussian noise commonly assumed in natural sciences and engineering. While Gaussian noise could be considered across the entire state space, how should we consider adversarial constraints?

In this study, we treat the search for the optimal adversary as an f -divergence constrained optimization problem, informed by the prior knowledge of perturbation distribution. From this, we derive two typical adversarial attacks: the Soft Worst-Case Attack (SofA) and the Epsilon Worst-Case (EpsA). To consider updates of the action-value function and the policy under such adversarial conditions, we have developed theoretically sound algorithms, from the perspective of contractions and policy improvements. At the conclusion of this introduction, we outline our contributions, which are twofold: by introducing f -divergence constrained methods, **(1)** we expand the application of robust DRL methods to recent innovative off-policy Actor-Critic algorithms, with a particular focus on the vulnerability that arises from MDPs, and **(2)** we introduce more arbitrary and realistic adversaries than those typically constrained by the conventional L_∞ -norm.

2 Related Work

2.1 Adversarial Attack and Defense on State Observations

Building on a seminal work by Goodfellow et al. [2014], there has been a surge of research activity in the field of supervised learning, particularly focusing on various adversarial attacks and corresponding defense methods [Kurakin et al., 2016, Papernot et al., 2016, 2017, Carlini and Wagner, 2017, Ilyas et al., 2018]. In the context of RL, Huang et al. [2017] demonstrated that similar challenges could arise from small perturbations, such as the Fast Gradient Sign Method (FGSM). This study led to the early proposal of various attacks on observations and corresponding robust methods [Kos and Song, 2017, Behzadan and Munir, 2017, Mandlekar et al., 2017, Pattanaik et al., 2018].

Recently, a line of research has focused on maintaining the consistency (smoothness) of the agent’s policy to acquire robustness against observation perturbations [Zhang et al., 2020, Shen et al., 2020, Oikarinen et al., 2021, Sun et al., 2024]. Zhang et al. [2020] first defined the adversarial observation problem as *State Adversarial Markov Decision Processes* (SA-MDPs). They proved and demonstrated that the loss in performance due to adversarial perturbations could be bounded by the consistency of the policy. However, in this study, they did not show practical methods to create the adversary that could estimate the long-term reward assumed in the SA-MDPs. Due to this gap, the proposed robust methods were not robust enough against stronger attacks [Zhang et al., 2021].

To address this issue, Zhang et al. [2021] proposed that the optimal (worst-case) adversary for the policy could be learned as a DRL agent. The policy, learned alternatively with such an adversary, can become robust against strong attacks (ATLA). Building on the ATLA framework, Sun et al. [2021] suggested dividing the adversary into two parts: searching for the mislead direction in the action space for the policy and calculating the actual perturbations in the state space through numerical approximation (PA-AD). This makes the adversary capable of handling high-dimensional state problems (such as Atari), which are difficult to address in the ATLA framework. These frameworks provide practical methods for on-policy algorithms (PPO, A2C), but applications for off-policy

algorithms were not shown. This is because the adversarial attacker learns from trajectories generated by the (current) fixed policy, but the policy is constantly updated during training.

Liang et al. [2022] introduced an additional worst-case action-value function to improve the policy’s robustness by utilizing a mixture with the original value function, referred to as *Worst-case-aware Robust* RL (WocaR-RL). This approach computes the worst-case action-value through convex relaxation and heuristic gradient iterations, thereby omitting additional environment steps, unlike ATLA-based methods (ATLA, PA-ATLA). WocaR-RL demonstrated effectiveness in high-dimensional discrete action domains using off-policy algorithms (e.g., DQN). However, applications for off-policy algorithms in continuous action domains were not shown and remain unknown.

As a separate line of research, there are studies that address the ratio and temporal strategies of attacks as a multi-agent problem [Lin et al., 2017, Gleave et al., 2019, Sun et al., 2020, Liu et al., 2024, Franzmeyer et al., 2024]. However, these studies focus on the objectives of time-step efficiency or the stealthiness of attacks. This motivation differs from our approach, which limits the attacker based on constraints from an assumed distribution.

3 Preliminaries and Background

Notations We describe the environment using a Markov Decision Process (MDP) characterized by parameters $\langle \mathcal{S}, \mathcal{A}, \mathcal{F}, r, \gamma, \mathcal{S}_0 \rangle$, where \mathcal{S} is the state space, \mathcal{A} is the action space, $\mathcal{F} : \mathcal{S} \times \mathcal{A} \rightarrow \Delta(\mathcal{S})$ defines the environment’s transition probabilities, where $\Delta(\mathcal{S})$ denotes the set of probability distributions over the state space \mathcal{S} , r is the reward function, γ is the discount factor, and \mathcal{S}_0 is the set of initial states. In RL framework, the objective is to find a policy $\pi(a|s) : \mathcal{S} \rightarrow \Delta(\mathcal{A})$ that maximizes the cumulative discounted reward along the trajectory, $\max_{\pi} \mathbb{E}_{\mathcal{S}_0, \pi, \mathcal{F}} [\sum_{t=0}^{\infty} \gamma^t r(s_t, a_t)]$. To reduce the variance in episodic trajectory estimates, RL maintains an action-value function $Q^{\pi}(s_t, a_t)$ and/or a state-value function $V^{\pi}(s_t)$.

3.1 Max-Entropy Off-Policy Actor Critic Algorithm

In this study, we utilize the Soft Actor Critic (SAC) [Haarnoja et al., 2018a,b] as our base algorithm. SAC is one of the most popular off-policy RL methods due to its theoretically sound foundations, sample-efficient, excellent performance, and simplicity. SAC assume a modified reward function:

$$\hat{r}(s_t, a_t) \triangleq r(s_t, a_t) + \mathbb{E}_{s_{t+1} \sim \mathcal{F}} [\alpha_{ent} \mathcal{H}(\pi(\cdot|s_{t+1}))], \quad (1)$$

where $\mathcal{H}(\pi(\cdot|s_{t+1}))$ represents the entropy term of the policy π for the state at time-step $t + 1$, and α_{ent} is an entropy coefficient to balance obtaining the original reward and encouraging exploration of actions.

Then, policy evaluation and improvement for π and Q^{π} are done as:

$$Q^{\pi}(s_t, a_t) = r(s_t, a_t) + \gamma \mathbb{E}_{s_{t+1} \sim \mathcal{F}} [\mathbb{E}_{a_{t+1} \sim \pi} [Q^{\pi}(s_{t+1}, a_{t+1}) - \alpha_{ent} \log \pi(a_{t+1}|s_{t+1})]], \quad (2)$$

$$L(\pi) = \mathbb{E}_{s_t \sim D(\cdot)} \left[D_{KL}(\pi(\cdot|s_t) \parallel \frac{\exp(Q^{\pi}(s_t, \cdot)/\alpha_{ent})}{\int_{a_t} \exp(Q^{\pi}(s_t, a_t)/\alpha_{ent}) da_t} \right), \quad (3)$$

where D_{KL} denotes Kullback-Leibler Divergence, and $D(\cdot)$ represents batch data from the replay buffer. By ignoring the constant term, we derive the final loss for the policy:

$$L(\pi) = \mathbb{E}_{s_t \sim D(\cdot)} [\mathbb{E}_{a_t \sim \pi} [\alpha_{ent} \log \pi(a_t|s_t) - Q^{\pi}(s_t, a_t)]]. \quad (4)$$

3.2 Reinforcement Learning under Adversarial Attack on State Observation

In scenarios with noisy observations, we consider adversarial perturbations $\nu(\tilde{s}_t|s_t) \in \mathcal{N}$, where $\mathcal{N} : \mathcal{S} \rightarrow \Delta(\mathcal{S})$ represents all possible perturbation functions mapping true state s_t to the set of probability over the state space \mathcal{S} . The perturbation occurs at each time step t , misleading the agent’s policy to output action \tilde{a}_t , while the environment dynamics transition to state s_{t+1} based on s_t and \tilde{a}_t . Crucially, **only the policy is deceived by the perturbation** $\nu(\tilde{s}_t|s_t)$, altering its action choice from $a_t \sim \pi(\cdot|s_t)$ to $\tilde{a}_t \sim \pi(\cdot|\tilde{s}_t)$. Previous research [Pattanaik et al., 2018, Zhang et al., 2020, 2021, Sun et al., 2021, Oikarinen et al., 2021, Liang et al., 2022] limits adversarial strength using an L_p -norm constraint (typically $p = \infty$), defining a restricted perturbation subset $\mathcal{B}_{\epsilon_p}(\nu; s_t) \subset \mathcal{N}$.

$$\mathcal{B}_{\epsilon_p}(\nu; s_t) := \{\nu_{\epsilon_p} \in \mathcal{N} : \nu_{\epsilon_p}(\tilde{s}_t|s_t) = 0 \text{ if } |\tilde{s}_t - s_t|_p > \epsilon, \text{ other } \nu_{\epsilon_p}(\tilde{s}_t|s_t) \geq 0\}. \quad (5)$$

If the expected action-value function is learned for the policy π and the policy is once fixed, then we can regard the optimal attacker problem for the policy as:

$$\nu_\pi^*(\tilde{s}_t|s_t) = \arg \min_{\nu \in \mathcal{B}_{\epsilon_p}(\nu; s_t)} \mathbb{E}_{\tilde{s}_t \sim \nu(\cdot|s_t)} \left[\mathbb{E}_{\tilde{a}_t \sim \pi(\cdot|\tilde{s}_t)} [Q^\pi(s_t, \tilde{a}_t)] \right], \quad (6)$$

where $Q^\pi(s, a) := \mathbb{E}_{\mathcal{F}, \tilde{a}_t \sim \pi \circ \nu} [\sum_{t=0}^{\infty} \gamma^t r(s_t, \tilde{a}_t) | s_0 = s, a_0 = a]$ is the action-value function learned under the corresponding perturbation ν . We will reconsider this restriction $\mathcal{B}_{\epsilon_p}(\nu; s_t)$ as the soft constrained problem in the next section.

4 Methodology

4.1 Soft Constrained Representation of Adversarial Attack on State Observation

To accommodate more flexible perturbation scenarios, we revisit Eq. (6), assuming prior knowledge of the perturbation distribution $p(\tilde{s}_t|s_t) \in \mathcal{N}$ in our target environment. We add a mild assumption that the adversarial attacker $\nu(\tilde{s}_t|s_t)$ aligns with the prior distribution¹, $\forall s_t, \tilde{s}_t \in \mathcal{S}$, if $\nu(\tilde{s}_t|s_t) > 0 \Rightarrow p(\tilde{s}_t|s_t) > 0$. This framework allows us to define the soft constrained optimal adversary:

Definition 1 (Soft Constrained Optimal Adversary on State Observation).

$$\nu_\pi^*(\tilde{s}_t|s_t) = \arg \min_{\nu \in \mathcal{N}} \mathbb{E}_{\tilde{s}_t \sim \nu} \left[\mathbb{E}_{\tilde{a}_t \sim \pi(\cdot|\tilde{s}_t)} [Q^\pi(s_t, \tilde{a}_t)] \right] + \alpha_{attk} D_f(\nu(\cdot|s_t) \| p(\cdot|s_t)). \quad (7)$$

Here, $D_f(\nu \| p)$ represents the general f -divergence between the perturbation distribution $\nu(\tilde{s}_t|s_t)$ and the prior distribution $p(\tilde{s}_t|s_t)$. α_{attk} is the coefficient term used to balance the worst action value and the constraints on the attacker distribution imposed by the prior knowledge distribution $p(\tilde{s}_t|s_t)$.

As discussed in Sun et al. [2021], using $Q^\pi(s_t, \tilde{a}_t)$ and $Q^\pi(s_t, \tilde{a}_t)$ in Eq. (7) differ from a strict perspective. $Q^\pi(s_t, \tilde{a}_t)$ can estimate the sequential effect of perturbation ν , while $Q^\pi(s_t, \tilde{a}_t)$ only estimates the one-step influence from ν . Then, using $Q^\pi(s_t, \tilde{a}_t)$ results in a stronger attacker by correctly estimating the long-term effects. However, from the attacker’s perspective, it is difficult to specify whether DRL methods account for robust frameworks or not. Therefore, we widely use $Q^\pi(s_t, \tilde{a}_t)$, even though it does not account for perturbations, for practical applicability.

Although various attackers can be characterized by specifying different f -divergences, in this study, we specifically propose two typical attacks, each detailed in subsequent subsections.

4.1.1 Soft Worst Attack (SofA) Sampling Method for the KL-divergence Constraint

When we set the f -divergence to KL-divergence, the optimal attacker for a fixed policy π and the corresponding action-value function Q^π can be derived by the Fenchel-Legendre transform (detailed in Appendix B.1) as follows:

$$\nu_\pi^{*soft}(\tilde{s}_t|s_t) = \frac{p(\tilde{s}_t|s_t) \exp(\mathbb{E}_{\tilde{a}_t \sim \pi(\cdot|\tilde{s}_t)} [-Q^\pi(s_t, \tilde{a}_t)/\alpha_{attk}])}{\int_{\tilde{s}_t} p(\tilde{s}_t|s_t) \exp(\mathbb{E}_{\tilde{a}_t \sim \pi(\cdot|\tilde{s}_t)} [-Q^\pi(s_t, \tilde{a}_t)/\alpha_{attk}]) d\tilde{s}_t}. \quad (8)$$

When dealing with continuous state and action spaces, direct access to this distribution is not possible. We can approximate this distribution using Markov Chain Monte Carlo (MCMC) or variational inference method; however, these methods require multiple accesses to the policy π and the action-value function Q^π to obtain even a single sample at each time-step t . To address this, we propose approximating a limited number (N) of samples using the prior knowledge distribution $p(\tilde{s}_t|s_t)$, and then adjusting the probability with importance weights:

$$\begin{aligned} \tilde{s}_{ti} &\sim p(\tilde{s}_t|s_t), \quad i = 1, 2, \dots, N, \\ \nu_\pi^{*soft}(\tilde{s}_t|s_t) &\simeq \nu_\pi^{*soft}(\tilde{s}_{ti}|s_t) \propto \frac{1}{p(\tilde{s}_{ti}|s_t)} \frac{p(\tilde{s}_{ti}|s_t) \exp(\mathbb{E}_{\tilde{a}_{ti} \sim \pi(\cdot|\tilde{s}_{ti})} [-Q^\pi(s_t, \tilde{a}_{ti})/\alpha_{attk}])}{\sum_{i=1}^N p(\tilde{s}_{ti}|s_t) \exp(\mathbb{E}_{\tilde{a}_{ti} \sim \pi(\cdot|\tilde{s}_{ti})} [-Q^\pi(s_t, \tilde{a}_{ti})/\alpha_{attk}])}, \quad (9) \\ &\propto \exp(\mathbb{E}_{\tilde{a}_{ti} \sim \pi(\cdot|\tilde{s}_{ti})} [-Q^\pi(s_t, \tilde{a}_{ti})/\alpha_{attk}]). \end{aligned}$$

¹This assumption is considered mild as it encompasses conventional L_p -norm constraints when $p(\tilde{s}_t|s_t)$ is defined as a uniform distribution within the L_p -norm ball.

This approximation is biased and of high variance, especially when the prior distribution $p(\tilde{s}_t|s_t)$ significantly deviates from the soft optimal adversary $\nu_\pi^{*soft}(\tilde{s}_t|s_t)$, or when the number of samples is insufficient to adequately represent $\nu_\pi^{*soft}(\tilde{s}_t|s_t)$. Despite these potential issues, the approximated distribution proves highly useful when interpreted as: **testing the noise $p(\tilde{s}_t|s_t)$ with N parallel samples at a time, then selecting a sample where the policy π performs suboptimally, with a soft weighted probability determined by the temperature parameter α_{attk}** . By selecting the number of samples N and adjusting the weakness parameter α_{attk} , we can simulate adversarial scenarios that realistically consider the frequency of pre-assumed noise, without being constrained to L_p -norm noise. We refer to this attacker as the Soft (worst) Attack (SofA) and explore its use for training and evaluation in Sections 4.2.1 and 5.1.1.

4.1.2 Epsilon Worst Approximation Attack (EpsA) for the α -divergence Constraint

Considering the case when the f -divergence in Eq.(7) is specified as the α -divergence, we can explore broader categories that encompass the SofA case (Section4.1.1). These α -divergence constraint problems tend to have more mode-seeking solutions as α decreases [Belousov and Peters, 2017, Xu et al., 2023]. Specifically, by setting $\alpha \ll 0$ and restricting the attacker’s distribution selection to a uniform distribution within the L_∞ -norm range with an attack scale ϵ , denoted as $\mathcal{U}(\tilde{s} | s - \epsilon, s + \epsilon)$, we can approximate the distribution by using the mode probability, denoted as κ_{worst} , as follows:

$$\nu_\epsilon^*(\tilde{s}|s) \simeq \begin{cases} \kappa_{worst} + \frac{1-\kappa_{worst}}{|\mathcal{S}_\epsilon|}, & \text{if } \tilde{s} = \arg \min_{\tilde{s}' \in \mathcal{B}_\epsilon} \mathbb{E}_{\tilde{a} \sim \pi(\cdot|\tilde{s}')} [Q^\pi(s, \tilde{a})], \\ \frac{1-\kappa_{worst}}{|\mathcal{S}_\epsilon|}, & \text{otherwise,} \end{cases} \quad (10)$$

where $|\mathcal{S}_\epsilon|$ represents the measure of the state space within the ϵ -bounded domain. The details of this approximation are discussed in Appendix C.1. Eq. (10) can be approximated by combining the uniform distribution with a numerical gradient approach, similar to the *Critic* attack [Pattanaik et al., 2018, Zhang et al., 2020]. We refer to this strategy as the Epsilon (worst) Attack (EpsA) and utilize it for training and evaluation in Sections 4.1.2 and 5.1.2.

4.2 Robust off-policy Reinforcement Learning via Soft Constrained Adversary

As the previous discussion, we introduced the two typical adversaries as the solution of the soft constrained dual problems. By defining the soft (epsilon) worst-attack action-value function for policy π as $Q^{\tilde{\pi}}(s, a) := \mathbb{E}_{\mathcal{F}, \tilde{a}_t \sim \pi \circ \nu} [\sum_{t=0}^{\infty} \gamma^t r(s_t, \tilde{a}_t) | s_0 = s, a_0 = a]$, we can propose two robust off-policy RL algorithms which assume the corresponding adversaries in the appropriate MDP manners. We should note that this framework is sample-efficient because it can work not only with off-policy algorithms but also does not require additional interaction with the environment for the adversary.

4.2.1 Soft Worst Max-Entropy Reinforcement Learning (SofA-SAC)

We assume the policy is degraded by the adversary, and therefore introduce an additional modification to the reward function in Eq. (1) as follows:

$$\hat{r}(s_t, a_t) \triangleq r(s_t, a_t) + \mathbb{E}_{s_{t+1} \sim \mathcal{F}} [\alpha_{ent} \mathcal{H}(\pi \circ \nu_{\pi_{ent}}^{*soft}(\cdot|s_{t+1}))]. \quad (11)$$

For simplicity, we define $V^{\tilde{\pi}}(s, \tilde{s}) := \mathbb{E}_{\tilde{a} \sim \pi} [Q(s, \tilde{a}) - \alpha_{ent} \log \pi(\tilde{a}|\tilde{s})]$, then we get the following soft worst attack for the max-entropy version:

$$\nu_{\pi_{ent}}^{*soft}(\tilde{s}_t|s_t) = \frac{p(\tilde{s}_t|s_t) \exp(-V^{\tilde{\pi}}(s_t, \tilde{s}_t)/\alpha_{attk})}{\int_{\tilde{s}_t} p(\tilde{s}_t|s_t) \exp(-V^{\tilde{\pi}}(s_t, \tilde{s}_t)/\alpha_{attk}) d\tilde{s}_t}. \quad (12)$$

Under such adversary, we can define the corresponding Bellman operator with a contraction property:

$$(\mathcal{T}_{soft}^\pi Q)(s_t, a_t) \triangleq r(s_t, a_t) + \gamma \mathbb{E}_{s_{t+1} \sim \mathcal{F}} \left[-\alpha_{attk} \log \left(\mathbb{E}_{\tilde{s}_{t+1} \sim p} \left[\exp(-V^{\tilde{\pi}}(s_{t+1}, \tilde{s}_{t+1})/\alpha_{attk}) \right] \right) \right]. \quad (13)$$

For the policy improvement, we consider the KL minimization problem under the adversary as:

$$\begin{aligned}
L(\pi) &= \mathbb{E}_{s_t \sim D(\cdot)} \left[D_{KL}(\pi \circ \nu_{\pi_{ent}, fixed}^{*soft}(\cdot | s_t) \parallel \frac{\exp(Q^\pi(s_t, \cdot) / \alpha_{ent})}{\int_{\tilde{a}_t} \exp(Q^\pi(s_t, \tilde{a}_t) / \alpha_{ent}) d\tilde{a}_t} \right) \\
&\propto \mathbb{E}_{s_t \sim D(\cdot)} \left[\mathbb{E}_{\tilde{s}_t \sim \nu_{\pi_{ent}, fixed}^{*soft}} \left[\mathbb{E}_{\tilde{a}_t \sim \pi} [\alpha_{ent} \log \pi(\tilde{a}_t | \tilde{s}_t) - Q^\pi(s_t, \tilde{a}_t)] \right] + const. \right] \\
&= \mathbb{E}_{s_t \sim D(\cdot)} \left[\mathbb{E}_{\tilde{s}_t \sim p} \left[\frac{\nu_{\pi_{ent}, fixed}^{*soft}(\tilde{s}_t | s_t)}{p(\tilde{s}_t | s_t)} \mathbb{E}_{\tilde{a}_t \sim \pi} [\alpha_{ent} \log \pi(\tilde{a}_t | \tilde{s}_t) - Q^\pi(s_t, \tilde{a}_t)] \right] \right],
\end{aligned} \tag{14}$$

where $\nu_{\pi_{ent}, fixed}^{*soft}$ denotes the (soft) optimal adversary that is fixed during policy improvement. We call this RL framework as the Soft (worst) Attack SAC (SofA-SAC). In the practical algorithm, we approximate using N samples for $\tilde{s}_t \sim p(\cdot | s_t)$. For a comprehensive derivation, theoretical validity properties (contraction and policy improvement), and detailed practical implementation, see Appendix B.3, B.4, and B.5.

4.2.2 Epsilon Worst Max-Entropy Reinforcement Learning (EpsA-SAC)

As in the previous subsection, we assume the policy is misled by the attack, then we consider the max-entropy version of the epsilon worst attack in Eq. (10) as:

$$\nu_{\pi_{ent}}^{*epsilon}(\tilde{s}_t | s_t) \simeq \begin{cases} \kappa_{worst} + \frac{1 - \kappa_{worst}}{|\mathcal{S}_\epsilon|}, & \text{if } \tilde{s} = \arg \min_{\tilde{s}' \in \mathcal{B}_\epsilon} \mathbb{E}_{\tilde{a} \sim \pi} [Q^\pi(s, \tilde{a}) - \alpha_{ent} \log \pi(\tilde{a} | \tilde{s}')] \\ \frac{1 - \kappa_{worst}}{|\mathcal{S}_\epsilon|}, & \text{otherwise} \end{cases}. \tag{15}$$

Under this perturbation, we define the epsilon-worst Bellman operator as:

$$\begin{aligned}
(\mathcal{T}_{epsilon}^\pi Q)(s_t, a_t) &\triangleq r(s_t, a_t) + \gamma \mathbb{E}_{s_{t+1} \sim \mathcal{F}} \left[\mathbb{E}_{\tilde{s}_{t+1} \sim \nu_{\pi_{ent}}^{*epsilon}} [V^{\tilde{\pi}}(s_{t+1}, \tilde{s}_{t+1})] \right] \\
&= r + \gamma \mathbb{E}_{s_{t+1} \sim \mathcal{F}} \left[\kappa_{worst} \mathbb{E}_{\tilde{s}_{t+1} \sim \nu_{\pi_{ent}}^{*worst}} [V^{\tilde{\pi}}(s_{t+1}, \tilde{s}_{t+1})] + (1 - \kappa_{worst}) \mathbb{E}_{\tilde{s}_{t+1} \sim \mathcal{U}_\epsilon} [V^{\tilde{\pi}}(s_{t+1}, \tilde{s}_{t+1})] \right].
\end{aligned} \tag{16}$$

For simplicity, we again use $V^{\tilde{\pi}}(s, \tilde{s}) := \mathbb{E}_{\tilde{a} \sim \pi} [Q(s, \tilde{a}) - \alpha_{ent} \log \pi(\tilde{a} | \tilde{s})]$. By considering the same divergence minimization problem in Eq. (14), we can improve the policy through:

$$\begin{aligned}
L(\pi) &= \mathbb{E}_{s_t \sim D} \left[\mathbb{E}_{\tilde{s}_t \sim \nu_{\pi_{ent}}^{*epsilon}} \left[\mathbb{E}_{\tilde{a}_t \sim \pi} [\alpha_{ent} \log \pi(\tilde{a}_t | \tilde{s}_t) - Q^\pi(s_t, \tilde{a}_t)] \right] \right] \\
&= \mathbb{E}_{s_t \sim D} \left[\kappa_{worst} \mathbb{E}_{\tilde{s}_t \sim \nu_{\pi_{ent}}^{*worst}} [-V^{\tilde{\pi}}(s_t, \tilde{s}_t)] + (1 - \kappa_{worst}) \mathbb{E}_{\tilde{s}_t \sim \mathcal{U}_\epsilon} [-V^{\tilde{\pi}}(s_t, \tilde{s}_t)] \right].
\end{aligned} \tag{17}$$

We refer to this RL framework as the Epsilon (worst) Attack SAC (EpsA-SAC). We can assert that this Bellman operator also possesses a contraction property under a fixed policy, and once the adversary is fixed, the policy can be improved monotonically. For detailed information, please see Appendix C.3. In Eq. (15), obtaining the analytical worst sample ($\tilde{s}_t \sim \nu_{\pi_{ent}}^{*worst}(\cdot | s_t)$) is infeasible when the environment comprises continuous states and actions. However, we have found that numerical approximations of the worst samples using the Critic attack [Pattanaik et al., 2018, Zhang et al., 2020] are practically effective. We employ the policy mean $\mu(\tilde{s}_t)$ and the action-value $Q^\pi(s_t, \tilde{a}_t)$, then apply gradient descent iteration to solve $\tilde{s}_t \simeq \arg \min_{\tilde{s}'_t \in \mathcal{B}_\epsilon} Q^\pi(s_t, \mu(\tilde{s}'_t))$ in subsequent experiments.

5 Experiments

In this section, we set up experiments to address the questions posed in the introduction: **(1)** Can we develop a robust **off-policy** algorithm that accounts for long-term rewards without requiring additional interactions? **(2)** Is it possible to incorporate more arbitrary distributions, based on prior knowledge, beyond the conventional L_p -norm constrained range, into both adversaries and defenses? Responses to **(1)** are addressed in Sections 5.1.1 and 5.1.2, and those to **(2)** are presented in Section 5.1.1.

Environments and Common settings We use four OpenAI Gym MuJoCo environments [Todorov et al., 2012]: Hopper, HalfCheetah, Walker2d, and Ant, as utilized in most prior works [Zhang et al., 2020, 2021, Oikarinen et al., 2021, Liang et al., 2022]. Detailed settings are documented in F.1.

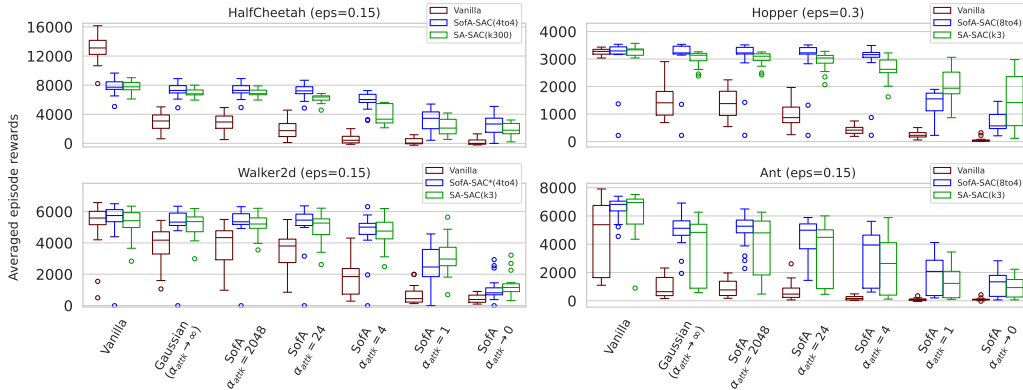


Figure 1: Robustness evaluation results of SofA-SAC and baseline algorithms under the Gaussian based attacks. Each boxplot depicts the 25%, 50%, and 75% percentile values of the mean returns.

Baselines and Implementations. We select the Soft Actor Critic (SAC) [Haarnoja et al., 2018a,b] as our base off-policy method and prepare our algorithms alongside two state-of-the-art robust algorithms for comparison, both of which potentially operate in an off-policy manner. First, the SAC version of SA-MDP [Zhang et al., 2020], referred to as *SA-SAC*, and second, the SAC version of Wocar [Liang et al., 2022], which we denote as *Wocar-SAC*. These comparisons aim to evaluate the performance capabilities of these algorithms under off-policy conditions. There is no provided code² for SAC-versions (off-policy) of SA-MDP, Wocar, nor evaluation methods, then we incorporate these methods into our implementation, followed by tuning hyper-parameters and settings appropriately. Wocar-SAC works well in small benchmarks (Pendulum, InvertedPendulum). However, we found that during training, as the attack scale increases, the policy suddenly degrades in performance due to the worst Q-value dropping too low in the four benchmarks. This occurred even when we used tighter bound convex-relaxation methods [Zhang et al., 2018, 2019] than the IBP [Gowal et al., 2018] used in the original Wocar implementation. More information for implementations and hyper-parameters are provided in Appendix F.1 for the base SAC, in Appendix F.2 for SofA-SAC, in Appendix F.4 for SA-SAC, and Appendix F.5 for Wocar-SAC.

5.1 Training and Evaluation

We have established two evaluation metrics for our analysis. The first metric aims to assess the effectiveness against adversaries not constrained by the L_p -norm, as discussed in Sections 4.1.1 and 4.2.1. The second metric evaluates the resilience of our methods against conventional strong attacks within the L_∞ -norm ball, detailed in Sections 4.1.2 and 4.2.2.

5.1.1 Evaluations of Soft Worst Case Scenarios under Gaussian-Based Attacks

Task Setup In this study, we use a Gaussian distribution as the prior knowledge perturbation $p(\tilde{s}_t|s_t)$, setting the standard deviations for the attack scales as $\sigma = 0.15, 0.30, 0.15, 0.15$ for HalfCheetah, Hopper, Walker2d, and Ant, respectively. We train the standard SAC (*Vanilla-SAC*), SA-SAC, and our proposed defense method SofA-SAC using identical training steps. Subsequently, we conduct evaluations under various attack settings.

We prepare four attack settings: one using the prior knowledge distribution (*Gaussian*) as-is, another applying our proposed method, denoted as SofA(α_{attk}), with varying degrees of adversarial preference parameter α_{attk} . Finally, for reference, we report results for the *MaxActionDiff (MAD)* [Zhang et al., 2020] and the *Critic* [Pattanaik et al., 2018, Zhang et al., 2020], where the standard deviation value serves as the noise constraint range in Appendix D. For the sampling approximation, we use $N = 64$ both for the evaluation attacker (SofA) and the proposal DRL methods (SofA-SAC). For SA-SAC and SofA-SAC training, we appropriately tune the coefficient terms that achieve robustness

²While SA-DDPG is implemented in Zhang et al. [2020], it appears that DDPG does not perform adequately on the four MuJoCo benchmarks.

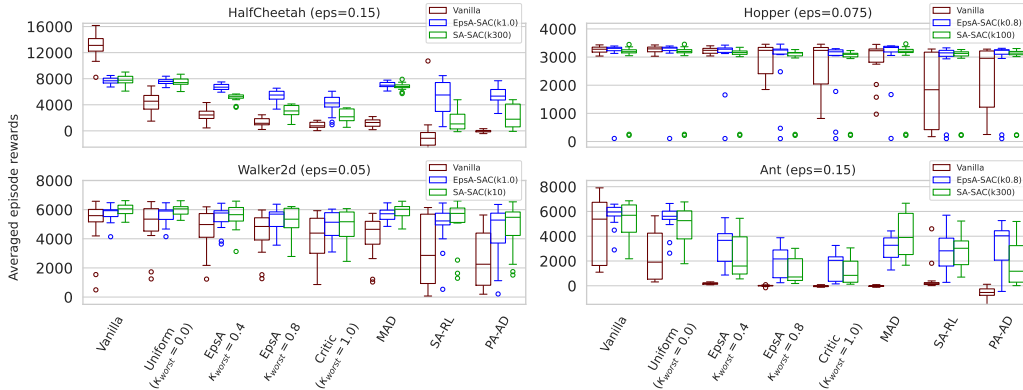


Figure 2: Robustness evaluation results of EpsA-SAC and baseline algorithms under the L_∞ -norm attacks. Each boxplot depicts the 25%, 50%, and 75% percentile values of the mean returns.

without compromising task performance (see Appendix D.3). For SofA-SAC, we maintain good performance and robustness across all tasks by $\alpha_{atk} = 4.0$ at the end of trainings, therefore, we consistently use this value. During tuning of the consistency parameter for SA-SAC, we find there is a trade-off between robustness and performance without attacks (see Appendix D.4), especially in HalfCheetah, as reported in Liang et al. [2022]. To compare under equal conditions, we tune the coefficient term of SA-SAC to achieve the same performance without attacks as SofA-SAC. Details of these hyperparameter settings are documented in Appendix F.2 and F.4.

Result Fig. 1 shows results of the robustness evaluation scores for Vanilla-SAC, our proposal method (SofA-SAC), and SA-SAC. As we estimated in Section 4.1.1, task scores drop as the attacker worst preference parameter (α_{atk}) approaches 0, here $\alpha_{atk} \rightarrow 0$ means worst sample pick-up. Though Vanilla-SAC drop its scores drastically, SofA-SAC and SA-SAC keep the performance even as the attacker gets stronger. Among all tasks, SofA-SAC keeps superior or competitive performance in the range of $\alpha_{atk} = [4.0, 2048.0]$ to SA-SAC, while inferior in the range of $[0.0, 1.0]$ for Hopper. In this study, SofA-SAC incorporates the attacked observation with the temperature parameter, $\alpha_{atk} = 4$ into the optimization problem during training, then stronger attack than this assumption may occur performance deterioration. Remarkably, both SofA-SAC and SA-SAC not only enhance robustness to observation noise but also consistently achieve high scores across multiple seeds. Therefore, we recommend these methods to the reader, except for tasks requiring conservative behavior where a trade-off between performance and robustness is necessary like in the HalfCheetah task.

5.1.2 Evaluations of Strong Attackers under Conventional L_∞ -norm Constraints

Task Setup For the robustness evaluation, we incorporate strong attackers as used in the most recent studies [Zhang et al., 2020, 2021, Sun et al., 2021, Oikarinen et al., 2021, Liang et al., 2022]. In addition to the conventional Random (Uniform), MAD, and Critic attacks, we include powerful attacks known as *SA-RL* [Zhang et al., 2021] and *PA-AD* [Sun et al., 2021] in our main evaluations. Furthermore, we introduce our proposed attack, EpsA (κ_{worst}), to examine robustness trends across different methods. We adopt the same attack scales as those commonly used in previous studies: $\epsilon = 0.15, 0.075, 0.05, 0.15$ for HalfCheetah, Hopper, Walker2d, and Ant, respectively.

For EpsA-SAC training, we find that increasing the worst ratio κ_{worst} from 0.0 to 0.8 or 1.0 during training works well, then we choose the one that is better in each task. As in Section 5.1.1, there is a trade-off between robustness and performance without attacks in some tasks (see Appendix 12). Then, we tune the coefficient term to achieve the same performance without attacks as EpsA-SAC does. Details of these hyperparameter settings are documented in Appendix F.3 and F.4.

Result Fig. 2 shows the evaluation results under the strong L_∞ -norm attackers. Especially in the more complex tasks (HalfCheetah, Ant) and strong attack evaluations (EpsA, Critic, SA-RL, PA-AD) that estimate long-term horizon, EpsA-SAC demonstrates superior or competitive performance

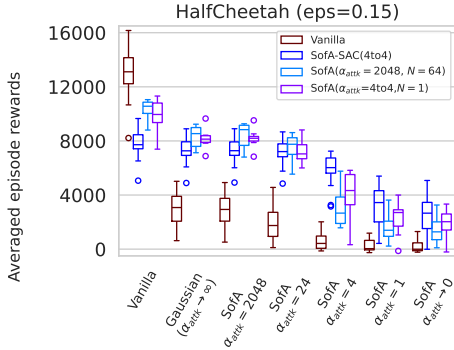


Figure 3: Ablation results for SofA-SAC’s hyperparameter. We change sample number and worst preference parameter, from $N = 64$ to 1 and from $\alpha_{attk} = 4$ to 2048.

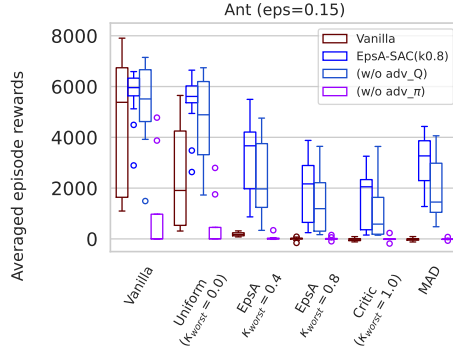


Figure 4: Ablation results for EpsA-SAC’s training strategy. We omit adversarial perturbation during policy improvement and Q updating in training.

compared to SA-SAC. In tasks with smaller perturbations (Walker), EpsA-SAC’s performance is competitive but slightly inferior to SA-SAC. We hypothesize that in tasks sensitive to small perturbations, simply maintaining consistent behaviors under these perturbations is more stable and preferable than comprehensive methods that account for MDPs under perturbations.

We should note that our results are based on the SAC implementation, not PPO, so the Q-function is trained according to the original method. Our DRL framework incorporates the adversarial effect into the Q-function, making the evaluation metrics that use such Q-functions much stronger. However, it is still superior to SA-SAC for the most tasks.

5.2 Ablation Studies

Due to limited space, we focus on the tasks where the influence of the hyperparameters and the effect of the adversaries during training are most apparent. Additional results, including other tasks and discussions, are documented in Appendices D and E.

SofA-SAC’s trade-off between performance and robustness Some readers may concern difference between SofA-SAC and SAC learning with just perturbed observation. Fig. 3 shows the confirmation result in HalfCheetah, by changing hyperparameter α_{attk} and sample number N . Learning with high temperature parameter, $\alpha_{attk} = 2048$, corresponding near averaged Gaussian perturbation, and $N = 1$ means using just sample from Gaussian distribution. Those both two variations result in relatively high performance without attacks than the reference, while less robustness under the stronger attack ($\alpha_{attk} \leq 24.0$). Therefore, we can say our SofA-SAC appropriately incorporates conservative behaviors that we assume at the training phase.

Importance of adversaries during policy improvement and action value update To analyze the effective factors of our learning framework, we conduct two variant trainings of EpsA-SAC. The one is lack of adversary during policy improvement, and the other is lack of adversary during action value update. Fig. 4 shows these ablation results. Without adversaries during Q-value updates, the results exhibit high variance and less robust performance, while the performance deteriorates when adversaries are absent during policy improvement. In the former case, the Q-function cannot adequately consider the pessimistic scenarios around the state s_t , and in the latter case, the policy fails to improve performance under attack, leading to low Q-values.

6 Conclusion and Future Work

We propose a new perspective on robust RL by introducing f-divergence constrained optimal adversaries with prior distributions. Our methods align naturally with theoretical expectations and demonstrate robust performance, particularly against strong attacks that comprehensively consider

MDPs. This framework offers a more flexible approach to designing robustness that closely aligns with real-world challenges and enhances the performance of off-policy algorithms.

For future work, we identify three main directions: developing a stronger algorithm that integrates functional smoothness; creating more efficient metrics for EpsA-SAC computation, as current methods rely heavily on gradient iterations for both policy evaluation and policy improvement; and extending this framework to other research domains, such as domain randomization.

7 Acknowledgements

We would like to express our gratitude to Satoshi Yamamori and Sotetsu Koyamada for their valuable advice on this research. We also extend our appreciation to all members of the Computer Science Domain at Honda R&D Co., especially to Ken Inuma, Akira Kanahara, and Kenji Goto, for their cooperation and understanding in supporting this research.

References

- Vahid Behzadan and Arslan Munir. Whatever does not kill deep reinforcement learning, makes it stronger. *arXiv preprint arXiv:1712.09344*, 2017.
- Boris Belousov and Jan Peters. f-divergence constrained policy improvement. *arXiv preprint arXiv:1801.00056*, 2017.
- Boris Belousov and Jan Peters. Entropic regularization of markov decision processes. *Entropy*, 21(7):674, 2019.
- Abdeslam Boularias, Jens Kober, and Jan Peters. Relative entropy inverse reinforcement learning. In *Proceedings of the fourteenth international conference on artificial intelligence and statistics*, pages 182–189. JMLR Workshop and Conference Proceedings, 2011.
- Stephen P Boyd and Lieven Vandenberghe. *Convex optimization*. Cambridge university press, 2004.
- Nicholas Carlini and David Wagner. Adversarial examples are not easily detected: Bypassing ten detection methods. In *Proceedings of the 10th ACM Workshop on Artificial Intelligence and Security*, pages 3–14, 2017.
- Roy Fox, Ari Pakman, and Naftali Tishby. Taming the noise in reinforcement learning via soft updates. *arXiv preprint arXiv:1512.08562*, 2015.
- Tim Franzmeyer, Stephen Marcus McAleer, Joao F. Henriques, Jakob Nicolaus Foerster, Philip Torr, Adel Bibi, and Christian Schroeder de Witt. Illusory attacks: Information-theoretic detectability matters in adversarial attacks. In *The Twelfth International Conference on Learning Representations*, 2024. URL <https://openreview.net/forum?id=F5dhGCdyYh>.
- Adam Gleave, Michael Dennis, Cody Wild, Neel Kant, Sergey Levine, and Stuart Russell. Adversarial policies: Attacking deep reinforcement learning. *arXiv preprint arXiv:1905.10615*, 2019.
- Ian Goodfellow, Jonathon Shlens, and Christian Szegedy. Explaining and harnessing adversarial examples. *JSME International Journal, Series 1: Solid Mechanics, Strength of Materials*, 33(4):468–473, 12 2014.
- Sven Gowal, Krishnamurthy Dvijotham, Robert Stanforth, Rudy Bunel, Chongli Qin, Jonathan Uesato, Relja Arandjelovic, Timothy Mann, and Pushmeet Kohli. On the effectiveness of interval bound propagation for training verifiably robust models. *arXiv preprint arXiv:1810.12715*, 2018.
- Tuomas Haarnoja, Haoran Tang, Pieter Abbeel, and Sergey Levine. Reinforcement learning with deep energy-based policies. In *International conference on machine learning*, pages 1352–1361. PMLR, 2017.
- Tuomas Haarnoja, Aurick Zhou, Pieter Abbeel, and Sergey Levine. Soft actor-critic: Off-policy maximum entropy deep reinforcement learning with a stochastic actor. In *International conference on machine learning*, pages 1861–1870. PMLR, 2018a.
- Tuomas Haarnoja, Aurick Zhou, Kristian Hartikainen, George Tucker, Sehoon Ha, Jie Tan, Vikash Kumar, Henry Zhu, Abhishek Gupta, Pieter Abbeel, et al. Soft actor-critic algorithms and applications. *arXiv preprint arXiv:1812.05905*, 2018b.
- Kaiming He, Xiangyu Zhang, Shaoqing Ren, and Jian Sun. Deep residual learning for image recognition. In *Proceedings of the IEEE conference on computer vision and pattern recognition*, pages 770–778, 2016.

- Sandy Huang, Nicolas Papernot, Ian Goodfellow, Yan Duan, and Pieter Abbeel. Adversarial attacks on neural network policies. *arXiv preprint arXiv:1702.02284*, 2017.
- Andrew Ilyas, Logan Engstrom, Anish Athalye, and Jessy Lin. Black-box adversarial attacks with limited queries and information. *35th International Conference on Machine Learning (ICML)*, 5, 2018.
- Geon-Hyeong Kim, Seokin Seo, Jongmin Lee, Wonseok Jeon, HyeongJoo Hwang, Hongseok Yang, and Kee-Eung Kim. Demodice: Offline imitation learning with supplementary imperfect demonstrations. In *International Conference on Learning Representations*, 2021.
- Geon-Hyeong Kim, Jongmin Lee, Youngsoo Jang, Hongseok Yang, and Kee-Eung Kim. Lobsdice: Offline learning from observation via stationary distribution correction estimation. *Advances in Neural Information Processing Systems*, 35:8252–8264, 2022.
- Diederik P Kingma and Jimmy Ba. Adam: A method for stochastic optimization. *arXiv preprint arXiv:1412.6980*, 2014.
- B Ravi Kiran, Ibrahim Sobh, Victor Talpaert, Patrick Mannion, Ahmad A Al Sallab, Senthil Yogamani, and Patrick Pérez. Deep reinforcement learning for autonomous driving: A survey. *IEEE Transactions on Intelligent Transportation Systems*, 23(6):4909–4926, 2021.
- Jens Kober, J Andrew Bagnell, and Jan Peters. Reinforcement learning in robotics: A survey. *The International Journal of Robotics Research*, 32(11):1238–1274, 2013.
- Jernej Kos and Dawn Song. Delving into adversarial attacks on deep policies. *arXiv preprint arXiv:1705.06452*, 2017.
- Ilya Kostrikov, Ofir Nachum, and Jonathan Tompson. Imitation learning via off-policy distribution matching. *arXiv preprint arXiv:1912.05032*, 2019.
- Alex Krizhevsky, Ilya Sutskever, and Geoffrey E Hinton. Imagenet classification with deep convolutional neural networks. *Advances in neural information processing systems*, 25, 2012.
- Alexey Kurakin, Ian Goodfellow, and Samy Bengio. Adversarial examples in the physical world. *arXiv preprint arXiv:1607.02533*, 2016.
- Sergey Levine, Chelsea Finn, Trevor Darrell, and Pieter Abbeel. End-to-end training of deep visuomotor policies. *The Journal of Machine Learning Research*, 17(1):1334–1373, 2016.
- Yongyuan Liang, Yanchao Sun, Ruijie Zheng, and Furong Huang. Efficient adversarial training without attacking: Worst-case-aware robust reinforcement learning. *Advances in Neural Information Processing Systems*, 35: 22547–22561, 2022.
- Yen-Chen Lin, Zhang-Wei Hong, Yuan-Hong Liao, Meng-Li Shih, Ming-Yu Liu, and Min Sun. Tactics of adversarial attack on deep reinforcement learning agents. *arXiv preprint arXiv:1703.06748*, 2017.
- Xiangyu Liu, Souradip Chakraborty, Yanchao Sun, and Furong Huang. Rethinking adversarial policies: A generalized attack formulation and provable defense in rl. 2024.
- Yecheng Ma, Andrew Shen, Dinesh Jayaraman, and Osbert Bastani. Versatile offline imitation from observations and examples via regularized state-occupancy matching. In *International Conference on Machine Learning*, pages 14639–14663. PMLR, 2022.
- Ajay Mandekar, Yuke Zhu, Animesh Garg, Li Fei-Fei, and Silvio Savarese. Adversarially robust policy learning: Active construction of physically-plausible perturbations. In *2017 IEEE/RSJ International Conference on Intelligent Robots and Systems (IROS)*, pages 3932–3939. IEEE, 2017.
- Volodymyr Mnih, Koray Kavukcuoglu, David Silver, Andrei A Rusu, Joel Veness, Marc G Bellemare, Alex Graves, Martin Riedmiller, Andreas K Fidjeland, Georg Ostrovski, et al. Human-level control through deep reinforcement learning. *Nature*, 518(7540):529–533, 2015.
- Ofir Nachum and Bo Dai. Reinforcement learning via fenchel-rockafellar duality. *arXiv preprint arXiv:2001.01866*, 2020.
- Tuomas Oikarinen, Wang Zhang, Alexandre Megretski, Luca Daniel, and Tsui-Wei Weng. Robust deep reinforcement learning through adversarial loss. *Advances in Neural Information Processing Systems*, 34: 26156–26167, 2021.

- Nicolas Papernot, Patrick McDaniel, Somesh Jha, Matt Fredrikson, Berkay-Z Celik, and Ananthram Swami. The limitations of deep learning in adversarial settings. In *2016 IEEE European symposium on security and privacy (EuroS&P)*, pages 372–387. IEEE, 2016.
- Nicolas Papernot, Patrick McDaniel, Ian Goodfellow, Somesh Jha, Berkay-Z Celik, and Ananthram Swami. Practical black-box attacks against machine learning. In *Proceedings of the 2017 ACM on Asia conference on computer and communications security*, pages 506–519, 2017.
- Anay Pattanaik, Zhenyi Tang, Shuijing Liu, Gautham Bommannan, and Girish Chowdhary. Robust deep reinforcement learning with adversarial attacks. *Proceedings of the International Joint Conference on Autonomous Agents and Multiagent Systems, AAMAS*, 3, 2018.
- Jan Peters, Katharina Mulling, and Yasemin Altun. Relative entropy policy search. In *Proceedings of the AAAI Conference on Artificial Intelligence*, volume 24, pages 1607–1612, 2010.
- Antonin Raffin, Ashley Hill, Adam Gleave, Anssi Kanervisto, Maximilian Ernestus, and Noah Dormann. Stable-baselines3: Reliable reinforcement learning implementations. *Journal of Machine Learning Research*, 22 (268):1–8, 2021. URL <http://jmlr.org/papers/v22/20-1364.html>.
- Tom Schaul, John Quan, Ioannis Antonoglou, and David Silver. Prioritized experience replay. *arXiv preprint arXiv:1511.05952*, 2015.
- John Schulman, Sergey Levine, Pieter Abbeel, Michael Jordan, and Philipp Moritz. Trust region policy optimization. In *International conference on machine learning*, pages 1889–1897. PMLR, 2015.
- John Schulman, Filip Wolski, Prafulla Dhariwal, Alec Radford, and Oleg Klimov. Proximal policy optimization algorithms. *arXiv preprint arXiv:1707.06347*, 2017.
- Qianli Shen, Yan Li, Haoming Jiang, Zhaoran Wang, and Tuo Zhao. Deep reinforcement learning with robust and smooth policy. In *International Conference on Machine Learning*, pages 8707–8718. PMLR, 2020.
- David Silver, Julian Schrittwieser, Karen Simonyan, Ioannis Antonoglou, Aja Huang, Arthur Guez, Thomas Hubert, Lucas Baker, Matthew Lai, Adrian Bolton, et al. Mastering the game of go without human knowledge. *Nature*, 550(7676):354–359, 2017.
- Karen Simonyan and Andrew Zisserman. Very deep convolutional networks for large-scale image recognition. *arXiv preprint arXiv:1409.1556*, 2014.
- Chung-En Sun, Sicun Gao, and Tsui-Wei Weng. Tactics of robust deep reinforcement learning with randomized smoothing, 2024. URL <https://openreview.net/forum?id=sRop0N5NYV>.
- Jianwen Sun, Tianwei Zhang, Xiaofei Xie, Lei Ma, Yan Zheng, Kangjie Chen, and Yang Liu. Stealthy and efficient adversarial attacks against deep reinforcement learning. In *Proceedings of the AAAI Conference on Artificial Intelligence*, volume 34, pages 5883–5891, 2020.
- Yanchao Sun, Ruijie Zheng, Yongyuan Liang, and Furong Huang. Who is the strongest enemy? towards optimal and efficient evasion attacks in deep rl. *arXiv preprint arXiv:2106.05087*, 2021.
- Richard S. Sutton and Andrew G. Barto. *Introduction to reinforcement learning*. MIT Press, 1998. URL <http://webdocs.cs.ualberta.ca/~sutton/book/ebook/the-book.html>, <http://webdocs.cs.ualberta.ca/~sutton/book/the-book.html>.
- Emanuel Todorov, Tom Erez, and Yuval Tassa. Mujoco: A physics engine for model-based control. In *2012 IEEE/RSJ International Conference on Intelligent Robots and Systems*, pages 5026–5033. IEEE, 2012. doi: 10.1109/IROS.2012.6386109.
- Haoran Xu, Li Jiang, Jianxiong Li, Zhuoran Yang, Zhaoran Wang, Victor Wai Kin Chan, and Xianyuan Zhan. Offline rl with no ood actions: In-sample learning via implicit value regularization. *arXiv preprint arXiv:2303.15810*, 2023.
- Kaidi Xu, Zhouxing Shi, Huan Zhang, Yihan Wang, Kai-Wei Chang, Minlie Huang, Bhavya Kailkhura, Xue Lin, and Cho-Jui Hsieh. Automatic perturbation analysis for scalable certified robustness and beyond. *Advances in Neural Information Processing Systems*, 33, 2020.
- Huan Zhang, Tsui-Wei Weng, Pin-Yu Chen, Cho-Jui Hsieh, and Luca Daniel. Efficient neural network robustness certification with general activation functions. *Advances in neural information processing systems*, 31, 2018.
- Huan Zhang, Hongge Chen, Chaowei Xiao, Sven Gowal, Robert Stanforth, Bo Li, Duane Boning, and Cho-Jui Hsieh. Towards stable and efficient training of verifiably robust neural networks. *arXiv preprint arXiv:1906.06316*, 2019.

Huan Zhang, Hongge Chen, Chaowei Xiao, Bo Li, Mingyan Liu, Duane Boning, and Cho-Jui Hsieh. Robust deep reinforcement learning against adversarial perturbations on state observations. *Advances in Neural Information Processing Systems*, 33:21024–21037, 2020.

Huan Zhang, Hongge Chen, Duane Boning, and Cho-Jui Hsieh. Robust reinforcement learning on state observations with learned optimal adversary. *arXiv preprint arXiv:2101.08452*, 2021.

APPENDIX

We describe additional related works, provide more detailed theoretical derivations, and offer additional evaluation results to help the reader gain a deeper understanding of our work. In the following, we temporarily set aside strict notation and represent expressions like " $\int_{a \in \mathcal{A}} \cdot, da$ " as " $\sum_{a \in \mathcal{A}} \cdot$ " when discussing continuous action space.

A Additional Related Works

A.1 f-Divergence Constrained Methods

The use of optimization methods constrained by f-divergence has spanned various contexts from historical applications to recent advancements. Historically, these methods were utilized for relative entropy maximization in inverse RL [Boularias et al., 2011]. In offline RL and imitation learning (IL), they primarily serve to constrain divergence from the probability density distribution of state-action pairs within the dataset [Xu et al., 2023, Kostrikov et al., 2019, Nachum and Dai, 2020, Kim et al., 2021, 2022, Ma et al., 2022]. Moreover, methods that limit update intervals by distribution constraints (old policy, prior) during policy updates [Peters et al., 2010, Fox et al., 2015, Schulman et al., 2015, 2017, Belousov and Peters, 2017, 2019] are closely related to our proposed soft-constrained adversary approach.

B Details of Soft Worst Attack (SofA) and SofA-SAC

B.1 Derivation of Soft Worst Attack (SofA)

We derive Eq. (8) from Eq. (7). At first, by flipping sign and converting arg min into arg max as:

$$\begin{aligned} \nu_{\pi}^{*soft}(\tilde{s}_t|s_t) &= \arg \min_{\nu \in \mathcal{N}} \mathbb{E}_{\tilde{s}_t \sim \nu(\cdot|s_t)} \left[\mathbb{E}_{\tilde{a}_t \sim \pi(\cdot|\tilde{s}_t)} [Q^{\pi}(s_t, \tilde{a}_t)] \right] + \alpha_{attk} D_f(\nu(\cdot|s_t) \| p(\cdot|s_t)) \\ &= - \arg \max_{\nu \in \mathcal{N}} \mathbb{E}_{\tilde{s}_t \sim \nu(\cdot|s_t)} \left[\mathbb{E}_{\tilde{a}_t \sim \pi(\cdot|\tilde{s}_t)} [(-Q^{\pi}(s_t, \tilde{a}_t))] \right] - \alpha_{attk} D_f(\nu(\cdot|s_t) \| p(\cdot|s_t)). \end{aligned} \quad (18)$$

Here, we only consider the KL-divergence case, then we derive:

$$\nu_{\pi}^{*soft}(\tilde{s}_t|s_t) = - \arg \max_{\nu \in \mathcal{N}} \mathbb{E}_{\tilde{s}_t \sim \nu(\cdot|s_t)} \left[\mathbb{E}_{\tilde{a}_t \sim \pi(\cdot|\tilde{s}_t)} [(-Q^{\pi}(s_t, \tilde{a}_t))] \right] - \alpha_{attk} D_{KL}(\nu(\cdot|s_t) \| p(\cdot|s_t)). \quad (19)$$

This type of optimization problem is often utilized in various context [Boyd and Vandenberghe, 2004, Peters et al., 2010, Boularias et al., 2011, Belousov and Peters, 2017], and there are two kinds of derivations, solving the Lagrangian with constraint or using the result of conjugate function of KL-divergence in the more general $f(\alpha)$ -divergence context. In this section, we describe the former type of derivation. This problem is described as follows:

$$\begin{aligned} \underset{\nu(\tilde{s}|s)}{\text{maximize}} \quad & \sum_{\tilde{s} \in \mathcal{S}} \underbrace{\nu(\tilde{s}|s)}_{\nu_{\tilde{s}}} \underbrace{\sum_{\tilde{a} \in \mathcal{A}} \pi(\tilde{a}|\tilde{s}) (-Q^{\pi}(s, \tilde{a}))}_{q_{\tilde{s}}} - \alpha_{attk} \sum_{\tilde{s} \in \mathcal{S}} \nu(\tilde{s}|s) (\log \nu(\tilde{s}|s) - \log p(\tilde{s}|s)) \\ & = \sum_{\tilde{s} \in \mathcal{S}} \nu_{\tilde{s}} q_{\tilde{s}} - \alpha_{attk} \sum_{\tilde{s} \in \mathcal{S}} \nu_{\tilde{s}} (\log \nu_{\tilde{s}} - \log p_{\tilde{s}}) := g(\boldsymbol{\nu}) \\ \text{subject to} \quad & \forall \tilde{s} \in \mathcal{S}, \quad \nu_{\tilde{s}} \geq 0, \\ & \sum_{\tilde{s} \in \mathcal{S}} \nu_{\tilde{s}} = 1. \end{aligned} \quad (20)$$

The Lagrangian function for this problem is given by³:

$$L(\boldsymbol{\nu}, \boldsymbol{\lambda}) = g(\boldsymbol{\nu}) + \lambda (1 - \sum_{\tilde{s} \in \mathcal{S}} \nu_{\tilde{s}}), \quad (21)$$

where λ is the Lagrange multiplier associated with the equality constraint. By rolling out the Karush-Kuhn-Tucker (KKT)'s stationary condition:

$$\begin{aligned} \nabla_{\boldsymbol{\nu}} g(\boldsymbol{\nu}) + \lambda \nabla_{\boldsymbol{\nu}} L(\boldsymbol{\nu}, \boldsymbol{\lambda}) &= \mathbf{0} \\ \rightarrow \forall \tilde{s} \in \mathcal{S}, \quad q_{\tilde{s}} - \alpha_{attk} (\log \nu_{\tilde{s}} - \log p_{\tilde{s}} + 1) - \lambda &= 0 \\ \rightarrow \log \nu_{\tilde{s}} &= \log p_{\tilde{s}} - 1 + \frac{q_{\tilde{s}} - \lambda}{\alpha_{attk}} \\ \rightarrow \nu_{\tilde{s}} &= p_{\tilde{s}} \exp(q_{\tilde{s}}/\alpha_{attk}) \exp(-\lambda/\alpha_{attk} - 1). \end{aligned} \quad (22)$$

³We abbreviate the inequality constraint because it can be vanished in Eq. (22)

Algorithm 1 Soft Worst Attack (SofA) Sampling Method

Input: state s_t , policy $\pi(a|s)$, action-value function $Q^\pi(s, a)$, temperature parameter α_{attk} , number of samples N , prior distribution function $p(\tilde{s}|s)$

Output: Soft worst sample \tilde{s}_t

- 1: **function** SOFA($s_t, \pi, Q^\pi, \alpha_{attk}, N, p$)
 - 2: Sample N times from the prior distribution $p(\tilde{s}|s)$:
 $\tilde{s}_{ti} \sim p(\tilde{s}|s_t)$ for $i = 1, 2, \dots, N$
 - 3: Estimate the action values for the perturbed states \tilde{s}_{ti} and policy $\pi(a|s)$:
 $\tilde{a}_{ti} \sim \pi(\cdot|\tilde{s}_{ti}), \tilde{Q}_{ti} = Q^\pi(s_t, \tilde{a}_{ti})$
 - 4: Calculate the probability of the Soft Worst Attack as in Eq. (9):
 $\nu(\tilde{s}_{ti}|s_t) = \frac{\exp(-\tilde{Q}_{ti}/\alpha_{attk})}{\sum_{j=1}^N \exp(-\tilde{Q}_{tj}/\alpha_{attk})}$
 - 5: Select one sample \tilde{s}_t from \tilde{s}_{ti} based on the calculated probability weights $\nu(\tilde{s}_{ti}|s_t)$:
 (if $\alpha_{attk} \rightarrow 0$, select $i = \arg \min_{i'} \tilde{Q}_{ti'}$)
 - 6: **return** \tilde{s}_t
 - 7: **end function**
-

By giving this result back into the equality constraint at Eq. (20), we can specify the Lagrange multiplier λ and optimal value for $\nu_{\tilde{s}}$:

$$\begin{aligned} \nu_{\tilde{s}}^* &= \nu^*(\tilde{s}|s) = \frac{p_{\tilde{s}} \exp(q_{\tilde{s}}/\alpha_{attk})}{\sum_{\tilde{s} \in \mathcal{S}} p_{\tilde{s}} \exp(q_{\tilde{s}}/\alpha_{attk})} \\ &= \frac{p(\tilde{s}|s) \exp\{\sum_{\tilde{a} \in \mathcal{A}} \pi(\tilde{a}|\tilde{s})(-Q^\pi(s, \tilde{a}))/\alpha_{attk}\}}{\sum_{\tilde{s} \in \mathcal{S}} p(\tilde{s}|s) \exp\{\sum_{\tilde{a} \in \mathcal{A}} \pi(\tilde{a}|\tilde{s})(-Q^\pi(s, \tilde{a}))/\alpha_{attk}\}}. \end{aligned} \quad (23)$$

This is the same equation as Eq. (8) and by giving ν^* back into $g(\nu)$, the optimal value is:

$$g(\nu^*) = \alpha_{attk} \log \sum_{\tilde{s} \in \mathcal{S}} p(\tilde{s}|s) \exp\left\{ \sum_{\tilde{a} \in \mathcal{A}} \pi(\tilde{a}|\tilde{s})(-Q^\pi(s, \tilde{a}))/\alpha_{attk} \right\}. \quad (24)$$

B.2 Procedure and Characteristics of Practical Soft Worst Attack (SofA)

To make clear vision of the practical soft worst attack, proposed in Section 4.1.1, we depict Algorithm1 as a pseudo code. When $N \rightarrow \infty$ and $\alpha_{attk} \rightarrow 0$, as in the line 5, $\tilde{s}_t \rightarrow \arg \min_{s' \in \text{supp}(p)} \mathbb{E}_{\tilde{a}_t \sim \pi(\cdot|s')} [Q(s_t, \tilde{a}_t)]$.

Therefore, this procedure can be seemed as a sampling based attack, while *Critic* attack [Pattanaik et al., 2018, Zhang et al., 2020] is the gradient iteration based attack. Compared to the Critic attack, this attack,

- (1) is gradient iteration free (not use back-propagation, forward two times), and can calculate N samples in parallel at once
- (2) can consider more flexible shape of adversary even when $\text{dom}(\nu(\tilde{s}|s))$ is not continuous, not differentiable
- (3) can incorporate realistic negative possibilities by choosing N and α_{attk}

In cases where the state space is as large as an image, it may not be possible to sample the worst-case scenarios, making this method unsuitable for situations where cyber attacks are anticipated. However, **in realistic engineering and development contexts, where noise is often assumed to follow a normal distribution, we believe that the characteristic (2) and (3) are considered to be very important.**

B.3 Derivation of Soft Worst Attack SAC (SofA-SAC)

In this subsection, we describe derivation of SofA-SAC in Section 4.2.1. We assume that the policy only knows perturbed states, then the input of its max-entropy objective \mathcal{H} is also perturbed as in Eq. (11). To think one step rollout, we can build modified Bellman equation associated with the Bellman operator as:

$$(\mathcal{T}_\nu^\pi Q)(s_t, a_t) \triangleq r(s_t, a_t) + \gamma \mathbb{E}_{s_{t+1} \sim \mathcal{F}} \left[\mathbb{E}_{\tilde{s}_{t+1} \sim \nu} \left[\mathbb{E}_{\tilde{a}_{t+1} \sim \pi} [Q(s_{t+1}, \tilde{a}_{t+1})] + \alpha_{ant} \mathcal{H}(\pi(\cdot|\tilde{s}_{t+1})) \right] \right]. \quad (25)$$

Now we think the policy π is fixed and the soft constrained optimal adversary:

$$\begin{aligned} (\mathcal{I}_{soft}^\pi Q)(s_t, a_t) &\triangleq r(s_t, a_t) + \gamma \mathbb{E}_{s_{t+1} \sim \mathcal{F}} \left[\right. \\ &\quad \left. \min_{\nu \in \mathcal{N}} \mathbb{E}_{\tilde{s}_{t+1} \sim \nu} \left[\mathbb{E}_{\tilde{a}_{t+1} \sim \pi} [Q(s_{t+1}, \tilde{a}_{t+1})] + \alpha_{ant} \mathcal{H}(\pi(\cdot|\tilde{s}_{t+1})) \right] + \alpha_{attk} D_{KL}(\nu \parallel p) \right]. \end{aligned} \quad (26)$$

The minimization problem in this equation can be solved similarly to Eq. (19) in Appendix B.1, by setting:

$$q_{\tilde{s}} \leftarrow \sum_{\tilde{a} \in \mathcal{A}} \pi(\tilde{a}|\tilde{s}) (- (Q(s, \tilde{a}) - \alpha_{ent} \log \pi(\tilde{a}|\tilde{s}))) \quad (27)$$

Substituting this term into Eq. (23) and Eq. (24), we derive Eq. (12) and Eq. (13).

For policy improvement, we consider the analytical solution to the maximization problem highlighted in the underlined part of Eq. (26):

$$\begin{aligned} \pi^*(a|\tilde{s}; s) &= \arg \max_{\pi'} \mathbb{E}_{\tilde{a} \sim \pi'(\cdot|\tilde{s})} [Q^\pi(s, \tilde{a})] + \alpha_{ent} \mathcal{H}(\pi'(\cdot|\tilde{s})) \\ &= \frac{\exp(Q^\pi(s, \tilde{a})/\alpha_{ent})}{\sum_{\tilde{a}' \in \mathcal{A}} \exp(Q^\pi(s, \tilde{a}')/\alpha_{ent})} \end{aligned} \quad (28)$$

This maximization problem is identical to the original Soft Q-learning [Haarnoja et al., 2017] and SAC papers [Haarnoja et al., 2018a,b], so we do not derive it here. Then, we think policy update with the perturbation,

$$\mathbb{E}_{\tilde{s} \sim \nu(\cdot|s)} [\pi_{new}(\tilde{a}|\tilde{s})] = (\pi_{new} \circ \nu)(\tilde{a}|\tilde{s}) \leftarrow \pi^*(\tilde{a}|\tilde{s}; s) = \frac{\exp\{Q^\pi(s, \tilde{a})/\alpha_{ent}\}}{Z} \quad (29)$$

Similar to the original SAC, this update is calculated by minimizing the KL-divergence between the left and right terms. Assuming the soft worst attacker $\nu_{\pi_{ent}}^*$ for ν , we derive Eq. (14).

B.4 Contraction and Policy Improvement Properties of SofA-SAC

Contraction Property To demonstrate the reliability of our proposed SofA-SAC algorithm, we discuss its contraction property in this subsection. We revisit the definition provided in Eq. (13):

$$\begin{aligned} \underline{T}_{soft}^\pi Q(s_t, a_t) &\triangleq r(s_t, a_t) - \gamma \mathbb{E}_{s_{t+1} \sim \mathcal{F}} [\alpha_{attk} \log (\mathbb{E}_{\tilde{s}_{t+1} \sim p} [\\ &\exp \left(\mathbb{E}_{\tilde{a}_{t+1} \sim \pi} \left[\frac{-(Q(s_{t+1}, \tilde{a}_{t+1}) - \alpha_{ent} \log \pi(\tilde{a}_{t+1}|\tilde{s}_{t+1}))}{\alpha_{attk}} \right] \right))]. \end{aligned} \quad (30)$$

Theorem 1. *The Soft Worst Bellman Operator \underline{T}_{soft}^π acts as a contraction operator for a fixed policy.*

Proof.

For simplicity in notation, we define:

$$f(Q(t)) \triangleq -\alpha_{attk} \log \sum_{\tilde{s}_t \in \mathcal{S}} p(\tilde{s}_t|s_t) \exp \left(- \sum_{\tilde{a}_t \in \mathcal{A}} \pi(\tilde{a}_t|\tilde{s}_t) (Q(s_t, \tilde{a}_t) - \alpha_{ent} \log \pi(\tilde{a}_t|\tilde{s}_t)) / \alpha_{attk} \right) \quad (31)$$

We assume there are two different action-value functions, $Q_1(s_t, a_t)$ and $Q_2(s_t, a_t)$, and as the same metric in G-learning [Fox et al., 2015] and Soft Q-learning [Haarnoja et al., 2017], we define $\epsilon = \|Q_1(s_t, a_t) - Q_2(s_t, a_t)\|_{s_t, a_t}$, here $\|\cdot\|_{s_t, a_t}$ denotes the max norm over s_t, a_t . Since $f(Q)$ is a monotonically increasing function for Q , then we can say:

$$\begin{aligned} \forall s_t, f(Q_1(t)) &\leq f(Q_2(t) + \epsilon) \\ &= -\alpha_{attk} \log \sum_{\tilde{s}_t \in \mathcal{S}} p(\tilde{s}_t|s_t) \exp \left(- \sum_{\tilde{a}_t \in \mathcal{A}} \pi(\tilde{a}_t|\tilde{s}_t) (Q_2(s_t, \tilde{a}_t) + \epsilon - \alpha_{ent} \log \pi(\tilde{a}_t|\tilde{s}_t)) / \alpha_{attk} \right) \\ &= -\alpha_{attk} \log \sum_{\tilde{s}_t \in \mathcal{S}} p(\tilde{s}_t|s_t) \exp \left(-\epsilon/\alpha_{attk} - \sum_{\tilde{a}_t \in \mathcal{A}} \pi(\tilde{a}_t|\tilde{s}_t) (Q_2(s_t, \tilde{a}_t) - \alpha_{ent} \log \pi(\tilde{a}_t|\tilde{s}_t)) / \alpha_{attk} \right) \\ &= \epsilon - \alpha_{attk} \log \sum_{\tilde{s}_t \in \mathcal{S}} p(\tilde{s}_t|s_t) \exp \left(- \sum_{\tilde{a}_t \in \mathcal{A}} \pi(\tilde{a}_t|\tilde{s}_t) (Q_2(s_t, \tilde{a}_t) - \alpha_{ent} \log \pi(\tilde{a}_t|\tilde{s}_t)) / \alpha_{attk} \right) \\ &= \|Q_1(s_t, a_t) - Q_2(s_t, a_t)\|_{s_t, a_t} + f(Q_2(t)) \\ &\leftrightarrow f(Q_1(t)) - f(Q_2(t)) \leq \|Q_1(s_t, a_t) - Q_2(s_t, a_t)\|_{s_t, a_t}. \end{aligned} \quad (32)$$

In the same way:

$$\begin{aligned} f(Q_1(t)) &\geq f(Q_2(t) - \epsilon) = f(Q_2(t)) - \|Q_1(s_t, a_t) - Q_2(s_t, a_t)\|_{s_t, a_t} \\ \Leftrightarrow f(Q_1(t)) - f(Q_2(t)) &\geq -\|Q_1(s_t, a_t) - Q_2(s_t, a_t)\|_{s_t, a_t}. \end{aligned} \quad (33)$$

Therefore, from the both inequalities, we derive:

$$\|f(Q_1(t)) - f(Q_2(t))\|_{s_t} \leq \|Q_1(s_t, a_t) - Q_2(s_t, a_t)\|_{s_t, a_t}. \quad (34)$$

Then, we consider difference between the two action-value functions after our Bellman operator:

$$\begin{aligned} \|\mathcal{T}_{soft}^\pi Q_1(s_t, a_t) - \mathcal{T}_{soft}^\pi Q_2(s_t, a_t)\|_{s_t, a_t} &= \|\gamma \mathbb{E}_{s_{t+1} \sim \mathcal{F}} [f(Q_1(t+1)) - f(Q_2(t+1))]\|_{s_t, a_t} \\ &\leq \gamma \|f(Q_1(t+1)) - f(Q_2(t+1))\|_{s_{t+1}} \\ &\stackrel{(34)}{\leq} \gamma \|Q_1(s_{t+1}, a_{t+1}) - Q_2(s_{t+1}, a_{t+1})\|_{s_{t+1}, a_{t+1}}. \end{aligned} \quad (35)$$

Therefore, we can say \mathcal{T}_{soft}^π is a contraction operator, because we perform this operation an infinite number of times, Q_1 and Q_2 converge to a fixed point. \square

Policy Improvement Property (with a fixed adversary) If we once fix the attacker ν , we can discuss the policy improvement theorem [Sutton and Barto, 1998] as the same manner in Haarnoja et al. [2017, 2018a,b]. For simplicity, we omit the entropy coefficient α_{ent} in this paragraph.

Theorem 2 (Policy Improvement Theorem with a Fixed Adversary). *Given a fixed adversary ν and a policy π , define a new policy $\hat{\pi}$ such that for all states s ,*

$$\hat{\pi} \circ \nu(\cdot | s) \propto \exp(Q_\nu^\pi(s, \cdot)). \quad (36)$$

Assuming that Q_ν^π and $\sum_{a \in \mathcal{A}} \exp(Q_\nu^\pi(s, a))$ are bounded for all s , it follows that $Q_\nu^{\hat{\pi}}(s, a) \geq Q_\nu^\pi(s, a)$ for all actions a and state s .

Proof.

If we extract a new policy $\hat{\pi}$ by using π and the corresponding action-value function Q_ν^π , a following equation holds:

$$\begin{aligned} \mathbb{E}_{\tilde{s} \sim \nu} [\mathcal{H}(\pi(\cdot | \tilde{s})) + \mathbb{E}_{\tilde{a} \sim \pi} [Q_\nu^\pi(s, \tilde{a})]] &\leq \mathbb{E}_{\tilde{s} \sim \nu} [\mathcal{H}(\hat{\pi}(\cdot | \tilde{s})) + \mathbb{E}_{\tilde{a} \sim \hat{\pi}} [Q_\nu^\pi(s, \tilde{a})]] \\ \Leftrightarrow \mathcal{H}(\pi \circ \nu(\cdot | s)) + \mathbb{E}_{\tilde{a} \sim \pi \circ \nu} [Q_\nu^\pi(s, \tilde{a})] &\leq \mathcal{H}(\hat{\pi} \circ \nu(\cdot | s)) + \mathbb{E}_{\tilde{a} \sim \hat{\pi} \circ \nu} [Q_\nu^\pi(s, \tilde{a})]. \end{aligned} \quad (37)$$

This is proven by:

$$\begin{aligned} D_{KL}(\pi \circ \nu(\cdot | s) \parallel \hat{\pi} \circ \nu(\cdot | s)) &= \sum_{\tilde{a} \in \mathcal{A}} \pi \circ \nu(\tilde{a} | s) (\log \pi \circ \nu(\tilde{a} | s) - \log \hat{\pi} \circ \nu(\tilde{a} | s)) \\ &= -\mathcal{H}(\pi \circ \nu(\cdot | s)) - \sum_{\tilde{a} \in \mathcal{A}} \pi \circ \nu(\tilde{a} | s) (\log \hat{\pi} \circ \nu(\tilde{a} | s)) \\ &= -\mathcal{H}(\pi \circ \nu(\cdot | s)) - \sum_{\tilde{a} \in \mathcal{A}} \pi \circ \nu(\tilde{a} | s) \left(Q_\nu^\pi(s, \tilde{a}) - \log \sum_{\tilde{a}' \in \mathcal{A}} \exp\{Q_\nu^\pi(s, \tilde{a}')\} \right) \\ &= -\mathcal{H}(\pi \circ \nu(\cdot | s)) - \mathbb{E}_{\tilde{a} \sim \pi \circ \nu(\cdot | s)} [Q_\nu^\pi(s, \tilde{a})] + \log \sum_{\tilde{a}' \in \mathcal{A}} \exp(Q_\nu^\pi(s, \tilde{a}')) \\ &= -[\text{LHS of (37)}] + [\text{RHS of (37)}] \geq 0. \end{aligned} \quad (38)$$

In the third equality, we used the result defined in Theorem2:

$$\hat{\pi} \circ \nu(\tilde{a} | s) = \frac{\exp Q_\nu^\pi(s, \tilde{a})}{\sum_{\tilde{a}' \in \mathcal{A}} \exp Q_\nu^\pi(s, \tilde{a}')}. \quad (39)$$

By using this result, we can confirm:

$$\begin{aligned} Q_\nu^\pi(s_t, \tilde{a}_t) &= r(s_t, \tilde{a}_t) + \gamma \mathbb{E}_{s_{t+1} \sim \mathcal{F}} [\mathbb{E}_{\tilde{s}_{t+1} \sim \nu} [\mathbb{E}_{\tilde{a}_{t+1} \sim \pi} [Q_\nu^\pi(s_{t+1}, \tilde{a}_{t+1})] + \mathcal{H}(\pi(\cdot | \tilde{s}_{t+1}))]] \\ &\leq r(s_t, \tilde{a}_t) + \gamma \mathbb{E}_{s_{t+1} \sim \mathcal{F}} [\underbrace{\mathbb{E}_{\tilde{s}_{t+1} \sim \nu} [\mathbb{E}_{\tilde{a}_{t+1} \sim \hat{\pi}} [Q_\nu^\pi(s_{t+1}, \tilde{a}_{t+1})]}_{\text{rollout}}] + \mathcal{H}(\hat{\pi}(\cdot | \tilde{s}_{t+1})))] \\ &\vdots \\ &\leq Q_\nu^{\hat{\pi}}(s_t, \tilde{a}_t). \end{aligned} \quad (40)$$

Then, under a fixed adversary ν , we can improve our policy $\pi \circ \nu$ by targeting Eq. (39). \square

As the discussion in Zhang et al. [2020], we cannot prove optimality for the resulting policy due to the adversary’s movement. However, we can train our algorithm (SofA-SAC) stably by pausing the adversary during the policy improvement, using the stop-gradient function as described in Eq. (14). This approach ensures stability in the training process.

B.5 Practical Implementation of SofA-SAC

Algorithm 2 presents a pseudocode representing the practical implementation of the SofA-SAC algorithm described in Section 4.2.1. In lines 5 and 6, $done_t$ is referred to as a binary flag indicating whether the task has ended at the end of step t . We basically follow learning process as in the original SAC [Haarnoja et al., 2018b], use two critic networks with target networks and one policy network without a target network. We find that, though SofA-SAC also estimate a target value for the critic in the pessimistic way, taking min value of the two critic outputs for the critic targets and the actor objectives is needed for stable learning.

Only in Walker2d, we observe that as the training proceeds, Q-values diverged in some seeds (about 2-3 seeds in 8 seeds), then we put two measures to stabilize only for Walker2d (line11, line16 in Algorithm 2) . This may be because Walker2d is a sensitive task and sometimes experiences drops in scores even when using Vanilla-SAC. We assume once some unintended large values from a DNN are used for updates, it cannot recover from the fallen states.

Algorithm 2 SofA-SAC Training

- 1: Initialize critic $Q_{\theta_{1,2}}(s, a)$ and actor $\pi_{\phi}(s)$
 - 2: Initialize target networks $Q_{\theta'_{1,2}}(s, a)$ by setting $\theta'_{1,2} \leftarrow \theta_{1,2}$
 - 3: Initialize a replay buffer $\mathcal{R} \leftarrow \emptyset$ and entropy coefficient $\alpha_{ent} \leftarrow 1.0$
 - 4: **for** $t = 1$ to T **do**
 - 5: Execute action $a_t \sim \pi_{\phi}(s_t)$, observe $(s_t, a_t, r_t, s_{t+1}, done_t)$, and store in \mathcal{R}
 - 6: Sample a mini-batch of M transitions $(s_t^i, a_t^i, r_t^i, s_{t+1}^i, done_t^i) \sim \mathcal{R}$
 - 7: **- Update Critic:**
 - 8: Sample N perturbed states $\tilde{s}_{t+1}^{ij} \sim p(\cdot | s_{t+1}^i)$ for each i
 - 9: Sample perturbed actions $\tilde{a}_{t+1}^{ij} \sim \pi(\cdot | \tilde{s}_{t+1}^{ij})$ for each ij
 - 10: Estimate target values for each sample:
 $v_{1,2}^{ij} = Q_{\theta'_{1,2}}(s_{t+1}^i, \tilde{a}_{t+1}^{ij}) - \alpha_{ent} \log \pi_{\phi}(\tilde{a}_{t+1}^{ij} | \tilde{s}_{t+1}^{ij})$
 - 11: Compute targets by averaging over N using log-sum-exp for stability:
 $y_{1,2}^i = r_t^i + (1 - done_t^i) \gamma \left(-\alpha_{attk} \log \frac{1}{N} \sum_{j=1}^N \exp \left(\frac{-v_{1,2}^{ij}}{\alpha_{attk}} \right) \right)$
 - 12: (- optional for Walker2d, clip $y_{1,2}^i$ by percentile values over N samples)
 - 13: Update $\theta_{1,2}$ by minimizing HuberLoss:
 $L(\theta_{1,2}) = \frac{1}{M} \sum_{i=1}^M L_{Hu}(Q_{\theta_{1,2}}(s_t^i, a_t^i), \min(y_{1,2}^i, y_{2,2}^i))$
 - 14: **- Update Actor:**
 - 15: Sample N perturbed states $\tilde{s}_t^{ij} \sim p(\cdot | s_t^i)$ for each i
 - 16: For each sample, sample actions for loss and importance weight calculation:
 $\tilde{a}_t^{ij}, \tilde{a}_t^{ij'} \sim \pi_{\phi}(\cdot | \tilde{s}_t^{ij})$
 - 17: Calculate loss and importance weight:
 $L^{ij} = \alpha_{ent} \log \pi_{\phi}(\tilde{a}_t^{ij} | \tilde{s}_t^{ij}) - \min_{\theta_{1,2}} Q_{\theta_{1,2}}(s_t^i, \tilde{a}_t^{ij})$
 $w^{ij} = \text{softmax}_{j'} \left(\left(\alpha_{ent} \log \pi_{\phi}(\tilde{a}_t^{ij'} | \tilde{s}_t^{ij}) - \text{mean}_{\theta_{1,2}} Q_{\theta_{1,2}}(s_t^i, \tilde{a}_t^{ij'}) \right) / \alpha_{attk} \right)$
 - 18: (- optional for Walker2d, ignore importance weight: $w^{ij} \leftarrow 1$)
 - 19: Update ϕ using policy loss and importance weight:
 $L(\phi) = \frac{1}{MN} \sum_{i=1}^M \sum_{j=1}^N sg(w^{ij}) \odot L^{ij}$
 - 20: **- Update Entropy Coefficient:**
 - 21: Re-use the entropy values during policy improvement and update α_{ent} :
 $\mathcal{H}_{current}^i = -\frac{1}{N} \sum_{j=1}^N \log \pi_{\phi}(\tilde{a}_t^{ij} | \tilde{s}_t^{ij})$
 $L(\alpha_{ent}) = -\frac{1}{M} \sum_{i=1}^M \alpha_{ent} (\mathcal{H}_{target} - \mathcal{H}_{current}^i)$
 - 22: **- Post Processing:**
 - 23: Soft update the target networks: $\theta'_{1,2} \leftarrow (1 - \tau)\theta'_{1,2} + \tau\theta_{1,2}$
 - 24: (-optional for Hopper and Ant, update the temperature α_{attk} according to the scheduling)
 - 25: **end for**
-

C Details of Epsilon Worst Attack (EpsA) and EpsA-SAC

C.1 Derivation (Approximation) of Epsilon Worst Attack (EpsA)

If we do not limit ourselves to only the KL-divergence case but consider a more general α -divergence in Definition 1, we can obtain a broader perspective on the worst-case attack. This approach is inspired by Belousov and Peters [2017, 2019], which provides more detail about the derivation and related perspectives on policy improvement.

An f -divergence is a measurements between two distribution and defined as:

$$D_f(\nu \parallel p) \triangleq \sum_{\tilde{s} \in \mathcal{S}} p(\tilde{s}|s) f\left(\frac{\nu(\tilde{s}|s)}{p(\tilde{s}|s)}\right) \quad (s \text{ is given}). \quad (41)$$

Here, $f(\cdot) : \Omega \rightarrow \mathbb{R}$ is a convex function with the properties, $\text{Range}(f) = (0, \infty)$ and $f(x') = 0 \Leftrightarrow x' = 1$. An α -divergence is a sub-family of the f -divergence that is defined as:

$$f_\alpha(x) \triangleq \frac{(x^\alpha - 1) - \alpha(x - 1)}{\alpha(\alpha - 1)} \quad (42)$$

The α -divergence includes many popular divergence: for example, the case, $\alpha \rightarrow 0$, results in Reverse-KL-divergence, $\alpha \rightarrow 1$ derive KL-divergence, and $\alpha = 2$ occurs (Pearson's) χ^2 -divergence. To solve dual problems, the convex conjugate function $f^*(y)$ for $f(x)$ is known to be useful. This is defined as:

$$f^*(y) = \sup_{x \in \text{dom}(f)} \{\langle y, x \rangle - f(x)\}, \quad (43)$$

where $\langle \cdot, \cdot \rangle$ denotes the inner dot product. If f and f^* are differentiable, by taking the derivative of Eq. (43), $\nabla_y f^*(y) = x^*$ and $\nabla_x \{\langle y, x \rangle - f(x)\}|_{x=x^*} = \mathbf{0}$, we obtain the property $(f^*)' = (f')^{-1}$.

For the α -divergence case, its conjugate function and the derivative function of the conjugate are:

$$f_\alpha^*(y) = \frac{1}{\alpha} (1 + (\alpha - 1)y)^{\frac{\alpha}{\alpha-1}} - \frac{1}{\alpha}, \quad (44)$$

$$(f_\alpha^*)'(y) = (1 + (\alpha - 1)y)^{\frac{1}{\alpha-1}}, \text{ for } (1 - \alpha)y < 1. \quad (45)$$

To consider the case described in Eq. (18), we can rewrite the problem as:

$$\begin{aligned} \underset{\nu(\tilde{s}|s)}{\text{maximize}} \quad & \sum_{\tilde{s} \in \mathcal{S}} \underbrace{\nu(\tilde{s}|s)}_{\nu_{\tilde{s}}} \underbrace{\sum_{\tilde{a} \in \mathcal{A}} \pi(\tilde{a}|\tilde{s}) (-Q^\pi(s, \tilde{a}))}_{q_{\tilde{s}}} - \alpha_{attk} \sum_{\tilde{s} \in \mathcal{S}} p(\tilde{s}|s) f_\alpha\left(\underbrace{\frac{\nu(\tilde{s}|s)}{p(\tilde{s}|s)}}_{\frac{\nu_{\tilde{s}}}{p_{\tilde{s}}}}\right) \\ & = \sum_{\tilde{s} \in \mathcal{S}} \nu_{\tilde{s}} q_{\tilde{s}} - \alpha_{attk} \sum_{\tilde{s} \in \mathcal{S}} p_{\tilde{s}} f_\alpha\left(\frac{\nu_{\tilde{s}}}{p_{\tilde{s}}}\right) := g(\boldsymbol{\nu}) \\ \text{subject to} \quad & \forall \tilde{s} \in \mathcal{S}, \quad \nu_{\tilde{s}} \geq 0, \\ & \sum_{\tilde{s} \in \mathcal{S}} \nu_{\tilde{s}} = 1. \end{aligned} \quad (46)$$

The Lagrangian for this problem is given by:

$$\begin{aligned} L(\boldsymbol{\nu}, \boldsymbol{\lambda}, \boldsymbol{\kappa}) &= g(\boldsymbol{\nu}) + \lambda(1 - \sum_{\tilde{s} \in \mathcal{S}} \nu_{\tilde{s}}) + \sum_{\tilde{s} \in \mathcal{S}} \kappa_{\tilde{s}} \nu_{\tilde{s}}, \\ \text{with the KKT's condition:} \quad & \forall \tilde{s} \in \mathcal{S}, \\ & \nabla_{\boldsymbol{\nu}} g(\boldsymbol{\nu}) - \lambda + \kappa_{\tilde{s}} = 0, \\ & \nu_{\tilde{s}} \geq 0, \\ & \kappa_{\tilde{s}} \nu_{\tilde{s}} = 0, \\ & \kappa_{\tilde{s}} \geq 0. \end{aligned} \quad (47)$$

Here, $\kappa_{\tilde{s}} := \kappa(\tilde{s}|s)$ represents the complementary slackness for the inequality constraint. From the stationarity condition, $\forall \tilde{s}$:

$$\begin{aligned} q_{\tilde{s}} - \alpha_{attk} f'_\alpha\left(\frac{\nu_{\tilde{s}}}{p_{\tilde{s}}}\right) - \lambda + \kappa_{\tilde{s}} &= 0 \\ \rightarrow f'_\alpha\left(\frac{\nu_{\tilde{s}}}{p_{\tilde{s}}}\right) &= \frac{q_{\tilde{s}} - \lambda + \kappa_{\tilde{s}}}{\alpha_{attk}} \rightarrow \nu_{\tilde{s}} = p_{\tilde{s}} (f'_\alpha)^{-1}\left(\frac{q_{\tilde{s}} - \lambda + \kappa_{\tilde{s}}}{\alpha_{attk}}\right). \end{aligned} \quad (48)$$

Then, using the property, where $(f^*)' = (f')^{-1}$, we derive the optimal $\nu_{\tilde{s}}$ as:

$$\nu^*(\tilde{s}|s) = p(\tilde{s}|s)(f_\alpha^*)' \left(\frac{\sum_{\tilde{a} \in \mathcal{A}} \pi(\tilde{a}|\tilde{s})(-Q^\pi(s, \tilde{a})) - \lambda^* + \kappa(\tilde{s}|s)}{\alpha_{attk}} \right). \quad (49)$$

This solution can be regarded as how to assign probability mass on the prior distribution $p(\tilde{s}|s)$ and it depends on $\pi, Q^\pi, \alpha_{attk}$, and α . If we assume only $\alpha < 1$ case, from Eq. (45), the term of $(f_\alpha^*)'$ must hold > 0 , then $p(\tilde{s}|s) > 0 \leftrightarrow \nu^*(\tilde{s}|s) > 0$ holds. From the complementary condition in Eq. (47), in this case, the slackness parameter $\kappa(s|\tilde{s})$ must be 0. And from the constraint in Eq. (45), we get the condition for λ :

$$\forall \tilde{s} \in \mathcal{S}, \lambda > \sum_{\tilde{a} \in \mathcal{A}} \pi(\tilde{a}|\tilde{s})(-Q^\pi(s, \tilde{a})) - \alpha_{attk} \frac{1}{1-\alpha}. \quad (50)$$

This inequality must hold for all \tilde{s} , thus in the case of maximum of the right term. Then, we define:

$$\lambda^* := \max_{\tilde{s}} \sum_{\tilde{a} \in \mathcal{A}} \pi(\tilde{a}|\tilde{s})(-Q^\pi(s, \tilde{a})) - \alpha_{attk} \frac{1}{1-\alpha} + \xi_\alpha, \quad (51)$$

where ξ_α is a residual that satisfies $\xi_\alpha > 0$. Considering the case if $\alpha \rightarrow -\infty$, the optimal value of constraint term approach the bound, $\lambda^* \rightarrow \max_{\tilde{s} \in \text{supp}(p)} \sum_{\tilde{a} \in \mathcal{A}} \pi(\tilde{a}|\tilde{s})(-Q^\pi(s, \tilde{a}))$. Therefore, ξ_α approaches to zero as $\alpha \rightarrow -\infty$. Substituting this back into Eq. (49) and setting $\xi(Q; \tilde{s}) := -\min_{\tilde{s} \in \text{supp}(p)} \sum_{\tilde{a} \in \mathcal{A}} \pi(\tilde{a}|\tilde{s})Q^\pi(s, \tilde{a}) + \sum_{\tilde{a} \in \mathcal{A}} \pi(\tilde{a}|\tilde{s})Q^\pi(s, \tilde{a})$, we can consider the cases where $\alpha \ll 0$ as follows:

$$\begin{aligned} \nu^*(\tilde{s}|s) &= p(\tilde{s}|s)(f_\alpha^*)' \left(\frac{-\xi(Q; \tilde{s}) + \alpha_{attk} \frac{1}{1-\alpha} - \xi_\alpha}{\alpha_{attk}} \right) \\ &= p(\tilde{s}|s) \left(\frac{1-\alpha}{\alpha_{attk}} (\xi_\alpha + \xi(Q^\pi; \tilde{s})) \right)^{\frac{1}{\alpha-1}} \\ &= p(\tilde{s}|s) \left(\frac{\alpha_{attk}}{1-\alpha} \frac{1}{\xi_\alpha + \xi(Q^\pi; \tilde{s})} \right)^{\frac{1}{1-\alpha}}. \end{aligned} \quad (52)$$

From this equation, we can determine that $\nu^*(\tilde{s}|s)$ exhibits a strong peak at $\xi(Q^\pi; \tilde{s}) = 0$, which corresponds to $\tilde{s}^* := \arg \min_{\tilde{s} \in \text{supp}(p)} (\sum_{\tilde{a} \in \mathcal{A}} \pi(\tilde{a}|\tilde{s})Q^\pi(s, \tilde{a}))$. It also shows a mild probability mass for

the other perturbation states due to the term of exponential, $0 < \frac{1}{1-\alpha} \ll 1$.

Now, we assume the prior $p(\tilde{s}|s)$ is the uniform distribution over L_∞ -norm constrained range. Then, we approximate the peak of the probability by a constant multiple of Dirac's delta function as $\kappa_{worst} \delta(\tilde{s}^*)$ and distribute the remaining probability equally as $1 - \kappa_{worst}$. We represent this approximation as:

$$\nu^*(\tilde{s}|s) \simeq \begin{cases} \kappa_{worst} + \frac{1-\kappa_{worst}}{|\mathcal{S}_\epsilon|}, & \text{if } \tilde{s} = \arg \min_{\tilde{s}' \in \mathcal{B}_\epsilon} \sum_{\tilde{a} \in \mathcal{A}} \pi(\tilde{a}|\tilde{s}')Q^\pi(s, \tilde{a}) \\ \frac{1-\kappa_{worst}}{|\mathcal{S}_\epsilon|}, & \text{others} \end{cases}. \quad (53)$$

C.2 Procedure of the Epsilon Worst Attack (EpsA)

We detail Algorithm 3 to clarify the procedure for utilizing the Epsilon Worst Attack (EpsA). Initially, we sample a value b from the uniform distribution $[0.0, 1.0)$. If $b < \kappa_{worst}$, we apply the Critic attack; conversely, if $b \geq \kappa_{worst}$, we apply a prior perturbation from the uniform distribution within the L_∞ -norm range. Although this attack is not conceptually new, essentially functioning as an ϵ -greedy strategy for the adversary, it facilitates the estimation of intermediate states between the worst-case scenario and the prior perturbation in a natural form. This method facilitates understanding scenarios where the worst-case occurs probabilistically and aids in integrating these adversarial elements into robust learning frameworks such as EpsA-SAC.

Algorithm 3 Epsilon Worst Attack (EpsA) Sampling Method

Input: state s_t , policy $\pi(a|s)$, action-value function $Q^\pi(s, a)$, worst rate parameter κ_{worst} , attack scale ϵ

Output: Epsilon worst sample \tilde{s}_t

- 1: **function** EPSA($s_t, \pi, Q^\pi, \kappa_{worst}, \epsilon$)
 - 2: Sample random value b from uniform distribution $[0.0, 1.0]$
 - 3: **if the case** $b < \kappa_{worst}$:
 - 4: Calculate the worst-case state as the same as the Critic attack:
 $\tilde{s}_t^{*new} \leftarrow \text{proj}(\tilde{s}_t^{*old} - \eta \frac{\partial \bar{Q}_\theta(s_t, \mu(\tilde{s}_t^{*old}))}{\partial \tilde{s}_t^{*old}})$,
 (η is step size, μ is a mean output of the policy π)
 - 5: **else:**
 - 6: Sample perturbed state from the uniform distribution in the L_∞ -normed ϵ range:
 $\tilde{s}_t \sim \mathcal{U}(\cdot | s_t - \epsilon, s_t + \epsilon)$
 - 7: **return** \tilde{s}_t
 - 8: **end function**
-

C.3 Contraction and Policy Improvement Properties of EpsA-SAC

Contraction Property To confirm the certainty of our proposal EpsA-SAC algorithm, we show the contraction property in this subsection. We recall the definition:

$$\begin{aligned} \underline{\mathcal{T}}_{\epsilon\text{psilon}}^\pi Q(s_t, a_t) \triangleq & r(s_t, a_t) + \gamma \mathbb{E}_{s_{t+1} \sim \mathcal{F}} [\\ & \underbrace{\kappa_{worst} \mathbb{E}_{\tilde{s}_{t+1}^* \sim \nu_{\pi_{ept}}^{*worst}} [\mathbb{E}_{\tilde{a}_{t+1}^* \sim \pi} [Q(s_{t+1}, \tilde{a}_{t+1}^*) - \alpha_{ent} \log \pi(\tilde{a}_{t+1}^* | \tilde{s}_{t+1}^*)]]}_{V_{worst}^\pi(s_{t+1})} \\ & + (1 - \kappa_{worst}) \underbrace{\mathbb{E}_{\tilde{s}_{t+1} \sim p} [\mathbb{E}_{\tilde{a}_{t+1} \sim \pi} [Q(s_{t+1}, \tilde{a}_{t+1}) - \alpha_{ent} \log \pi(\tilde{a}_{t+1} | \tilde{s}_{t+1})]]}_{V_p^\pi(s_{t+1})} \\ &] \end{aligned} \quad (54)$$

Theorem 3. The Epsilon Worst Bellman Operator $\underline{\mathcal{T}}_{\epsilon\text{psilon}}^\pi$ is a contraction operator for a fixed policy.

Proof.

We should remind the fact from the definition of the epsilon worst-case:

$$V_{worst}^\pi(s_{t+1}) = \min_{\tilde{s}_{t+1}^* \in \mathcal{B}_{\epsilon p}(s_{t+1})} \mathbb{E}_{\tilde{a}_{t+1}^* \sim \pi} [Q(s_{t+1}, \tilde{a}_{t+1}^*) - \alpha_{ent} \log \pi(\tilde{a}_{t+1}^* | \tilde{s}_{t+1}^*)]. \quad (55)$$

Then, we consider difference between two action-value functions, Q_1, Q_2 , after using the Epsilon Worst Bellman operator:

$$\begin{aligned} & \|\underline{\mathcal{T}}_{\epsilon\text{psilon}}^\pi Q_1(s_t, a_t) - \underline{\mathcal{T}}_{\epsilon\text{psilon}}^\pi Q_2(s_t, a_t)\|_{s_t, a_t} \\ &= \|\gamma \mathbb{E}_{s_{t+1} \sim \mathcal{F}} [\kappa V_{1, worst}^\pi + (1 - \kappa) V_{1, p}^\pi - \kappa V_{2, worst}^\pi - (1 - \kappa) V_{2, p}^\pi]\|_{s_t, a_t} \\ &\leq \gamma \kappa \|\mathbb{E}_{s_{t+1} \sim \mathcal{F}} [V_{1, worst}^\pi - V_{2, worst}^\pi]\|_{s_t, a_t} + \gamma(1 - \kappa) \|\mathbb{E}_{s_{t+1} \sim \mathcal{F}} [V_{1, p}^\pi - V_{2, p}^\pi]\|_{s_t, a_t} \\ &\stackrel{(1)}{\leq} \gamma \kappa \|\mathbb{E}_{s_{t+1} \sim \mathcal{F}} [V_{1, worst}^\pi - V_{2, worst}^\pi]\|_{s_t, a_t} + \gamma(1 - \kappa) \|Q_1 - Q_2\|_{s_{t+1}, a_{t+1}} \\ &\stackrel{(2)}{\leq} \gamma \kappa \|Q_1 - Q_2\|_{s_{t+1}, a_{t+1}} + \gamma(1 - \kappa) \|Q_1 - Q_2\|_{s_{t+1}, a_{t+1}} \\ &= \gamma \|Q_1(s_{t+1}, a_{t+1}) - Q_2(s_{t+1}, a_{t+1})\|_{s_{t+1}, a_{t+1}}. \end{aligned} \quad (56)$$

For the inequality (1), we cancel entropy terms (under the same policy and perturbation) and use:

$$\mathbb{E}_{\tilde{s}_{t+1} \sim p} [\mathbb{E}_{\tilde{a}_{t+1} \sim \pi} [Q_1(s_{t+1}, \tilde{a}_{t+1}) - Q_2(s_{t+1}, \tilde{a}_{t+1})]] \leq \|Q_1(s_{t+1}, \tilde{a}_{t+1}) - Q_2(s_{t+1}, \tilde{a}_{t+1})\|_{a_{t+1}}. \quad (57)$$

For the inequality (2), similarly to the WocaR case [Liang et al., 2022], we utilized:

$$|\min_{\tilde{s} \in \mathcal{B}} A - \min_{\tilde{s} \in \mathcal{B}} B| \leq \max_{\tilde{s} \in \mathcal{B}} |A - B| \quad (58)$$

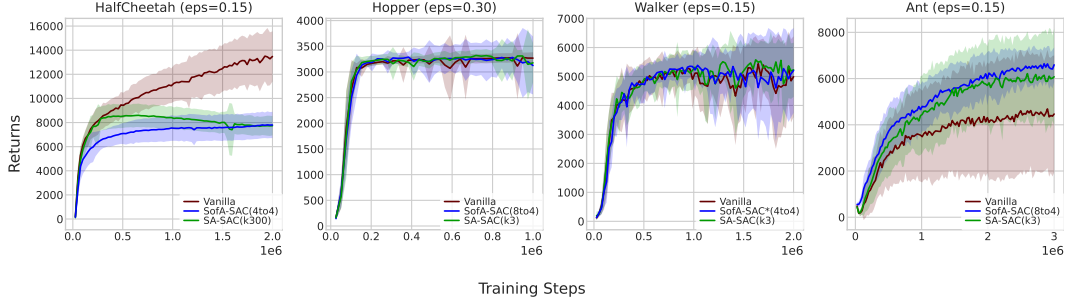


Figure 5: Learning curves for SofA-SAC and baseline algorithms on four MuJoCo control tasks. The solid lines represent the average evaluation scores, and the shaded areas indicate the standard deviation.

and canceling entropy terms due to the same fixed policy.

Therefore, we can say $\mathcal{T}_{\epsilon}^{\pi}$ is a contraction operator, because we perform this operation an infinite number of times, Q_1 and Q_2 converge to a fixed point. \square

Policy Improvement Property (with a fixed adversary) We can also say EpsA-SAC can improve the policy under a fixed adversary. Derivation is perfectly same as for SofA-SAC in Appendix B.4, then we omit the description here. We should note that in Eq. (17), we approximate $\tilde{s}_t \sim \nu_{\pi_{ent}}^{*worst}(\cdot|s_t)$ by the numerical method, Projected Gradient Descent (PGD), then naturally we fix the adversary during updating the policy.

C.4 Practical Implementation of EpsA-SAC

Algorithm 4 shows a pseudocode that represents practical implementation of the EpsA-SAC algorithm in Section 4.2.2. As for the same reason as in SofA-SA, we use two critic networks with target networks and one policy network without a target network.

Compared to SofA-SAC, without any special measurements, EpsA-SAC can train agents stably among all the four tasks by gradually increasing the worst-case weight κ_{worst} from 0.0 to the final value (most case we found $\{0.8, 1.0\}$ is preferable).

D Additional Results and Experiments for SofA-SAC

In this section, we present the results of additional experiments to detail the characteristics of SofA-SAC and validate the observed tendencies.

D.1 Learning Curves and Evaluation Score Tables for SofA-SAC and Baseline Algorithms

Fig. 5 presents the learning curves for SofA-SAC and baseline algorithms in Section 5.1.1. We would like to remind you that during training, SofA-SAC utilized Gaussian-based observation perturbations (virtually), and SA-SAC maintained the consistency of the policy output under the L_{∞} -norm. However, the actual trainings were executed without any perturbation. Although we observe modest scores due to enhanced robustness in HalfCheetah, we found that the introduction of SofA-SAC and SA-SAC did not sacrifice performance. Furthermore, learnings were more stable than with Vanilla-SAC in the complex task (Ant).

Table 1 shows the median values of average evaluation scores obtained from sixteen different training seeds. Notably, the scores of Vanilla-SAC decrease significantly as the temperature parameter α_{atk} is reduced. In contrast, our proposed method maintains performance and outperforms other baseline models, especially when $\alpha_{atk} \geq 4$.

Following the recommendation in Zhang et al. [2021], which suggests choosing the median seeds from the evaluation where the methods get the weakest scores, we attempt to extract median seeds. However, we observe that ranking scores under the strongest attack conditions occasionally results in selecting training seeds that perform significantly worse in attack-free evaluations. This issue is

Algorithm 4 EpsA-SAC Training

- 1: Initialize critic $Q_{\theta_{1,2}}(s, a)$ and actor $\pi_\phi(s)$
 - 2: Initialize target networks $Q_{\theta'_{1,2}}(s, a)$ by setting $\theta'_{1,2} \leftarrow \theta_{1,2}$
 - 3: Initialize a replay buffer $\mathcal{R} \leftarrow \emptyset$ and entropy coefficient $\alpha_{ent} \leftarrow 1.0$
 - 4: **for** $t = 1$ to T **do**
 - 5: Execute action $a_t \sim \pi_\phi(s_t)$, observe $(s_t, a_t, r_t, s_{t+1}, done_t)$, and store in \mathcal{R}
 - 6: Sample a mini-batch of M transitions $(s_t^i, a_t^i, r_t^i, s_{t+1}^i, done_t^i) \sim \mathcal{R}$
 - 7: **- Update Critic:**
 - 8: **- For random-case adversaries:**
 - 9: Sample perturbed states from the uniform distribution:
 $\tilde{s}_{t+1}^i \sim \mathcal{U}(\cdot | s_{t+1}^i - \epsilon, s_{t+1}^i + \epsilon)$
 - 10: Estimate random-case target values for each sample:
 $\tilde{a}_{t+1}^i \sim \pi_\phi(\cdot | \tilde{s}_{t+1}^i), \quad v_{1,2}^{ir} = Q_{\theta'_{1,2}}(s_{t+1}^i, \tilde{a}_{t+1}^i) - \alpha_{ent} \log \pi_\phi(\tilde{a}_{t+1}^i | \tilde{s}_{t+1}^i)$
 $y^{ir} = r_t^i + (1 - done_t^i) \gamma \min_{\{1,2\}} v_{1,2}^{ir}$
 - 11: **- For worst-case adversaries:**
 - 12: Compute worst-case states \tilde{s}_{t+1}^{i*} by using PGD in the L_∞ -norm state space (5 steps):
 $\tilde{s}_{t+1}^{i*new} \leftarrow \text{proj}(\tilde{s}_{t+1}^{i*old} - \eta \frac{\partial Q_{\theta'_{1,2}}(s_{t+1}^i, \mu(\tilde{s}_{t+1}^{i*old}))}{\partial \tilde{s}_{t+1}^{i*old}}), \eta$: step size, μ : mean action
 - 13: Estimate worst-case target values for each sample:
 $\tilde{a}_{t+1}^{i*} \sim \pi_\phi(\cdot | \tilde{s}_{t+1}^{i*}), \quad v_{1,2}^{i*} = Q_{\theta'_{1,2}}(s_{t+1}^i, \tilde{a}_{t+1}^{i*}) - \alpha_{ent} \log \pi_\phi(\tilde{a}_{t+1}^{i*} | \tilde{s}_{t+1}^{i*})$
 $y^{i*} = r_t^i + (1 - done_t^i) \gamma \min_{\{1,2\}} v_{1,2}^{i*}$
 - 14: Update $\theta_{1,2}$ by minimizing Huber-Loss:
 $L(\theta_{1,2}) = \frac{1}{M} \sum_{i=1}^M (\kappa_{worst} L_{\text{Hu}}(Q_{\theta_{1,2}}(s_t^i, a_t^i), y^{i*}) + (1 - \kappa_{worst}) L_{\text{Hu}}(Q_{\theta_{1,2}}(s_t^i, a_t^i), y^{ir}))$
 - 15: **- Update Actor:**
 - 16: **- For random-case adversaries:**
 - 17: Sample perturbed states from the uniform distribution:
 $\tilde{s}_t^i \sim \mathcal{U}(\cdot | s_t^i - \epsilon, s_t^i + \epsilon)$
 - 18: Calculate loss for the policy:
 $\tilde{a}_t^{ir} \sim \pi_\phi(\cdot | \tilde{s}_t^{ir}),$
 $L^{ir} = \alpha_{ent} \log \pi_\phi(\tilde{a}_t^{ir} | \tilde{s}_t^{ir}) - \min_{\theta_1, \theta_2} Q_{\theta_{1,2}}(s_t^i, \tilde{a}_t^{ir})$
 - 19: **- For worst-case adversaries:**
 - 20: Compute worst-case states \tilde{s}_t^{i*} by using PGD in the L_∞ -norm state space (5 steps):
 $\tilde{s}_t^{i*new} \leftarrow \text{proj}(\tilde{s}_t^{i*old} - \eta \frac{\partial Q_{\theta_{1,2}}(s_t^i, \mu(\tilde{s}_t^{i*old}))}{\partial \tilde{s}_t^{i*old}}), \eta$: step size, μ : action mean
 - 21: Calculate loss for the policy:
 $\tilde{a}_t^{i*} \sim \pi_\phi(\cdot | \tilde{s}_t^{i*}),$
 $L^{i*} = \alpha_{ent} \log \pi_\phi(\tilde{a}_t^{i*} | \tilde{s}_t^{i*}) - \min_{\theta_1, \theta_2} Q_{\theta_{1,2}}(s_t^i, \tilde{a}_t^{i*})$
 - 22: Update ϕ by minimizing mixed policy loss:
 $L(\phi) = \frac{1}{M} \sum_{i=1}^M (\kappa_{worst} L^{i*} + (1 - \kappa_{worst}) L^{ir})$
 - 23: **- Update Entropy Coefficient:**
 - 24: Re-use the entropy values during policy improvement and update α_{ent} :
 $\mathcal{H}_{current}^i = -\kappa_{worst} \log \pi_\phi(\tilde{a}_t^{i*} | \tilde{s}_t^{i*}) - (1 - \kappa_{worst}) \log \pi_\phi(\tilde{a}_t^{ir} | \tilde{s}_t^{ir})$
 $L(\alpha_{ent}) = -\frac{1}{M} \sum_{i=1}^M \alpha_{ent} (\mathcal{H}_{target}^i - \mathcal{H}_{current}^i)$
 - 25: **- Post Processing:**
 - 26: Soft update the target networks: $\theta'_{1,2} \leftarrow (1 - \tau)\theta'_{1,2} + \tau\theta_{1,2}$
 - 27: Update the worst-case weight parameter κ_{worst} according to the schedule
 - 28: **end for**
-

particularly pronounced with Vanilla-SAC, which sometimes fails to achieve valid scores during strong attack evaluations. Therefore, we represent all the averaged evaluation scores in the box plots for each method and evaluation, this can represent the variance and tendencies each methods have.

Table 1: Median values of average episode rewards across 16 different seed models of original SAC, SA-SAC, and SofA-SAC for four MuJoCo control tasks. Bold scores indicate the highest evaluation scores among the three methods.

Environment	Method	Vanilla	Gaussian ($\alpha_{\text{atk}} \rightarrow \infty$)	SofA $\alpha_{\text{atk}} = 2048$	SofA $\alpha_{\text{atk}} = 24$	SofA $\alpha_{\text{atk}} = 4$	SofA $\alpha_{\text{atk}} = 1$	SofA $\alpha_{\text{atk}} \rightarrow 0$
HalfCheetah $\epsilon = 0.15$	Vanilla	13110.6	3075.6	2934.9	1746.7	422.7	37.9	-8.4
	SA-SAC	7769.3	6810.6	6832.1	6369.4	3320.8	2096.4	1804.1
	SofA-SAC (Ours)	7720.5	7268.5	7278.2	7212.1	6025.6	3443.8	2659.9
Hopper $\epsilon = 0.30$	Vanilla	3278.2	1408.0	1378.7	868.6	414.2	224.6	20.3
	SA-SAC	3334.3	3137.9	3102.3	3039.0	2625.8	1937.8	1415.9
	SofA-SAC (Ours)	3293.8	3221.3	3221.4	3225.3	3159.6	1551.2	567.8
Walker2d $\epsilon = 0.15$	Vanilla	5587.6	4172.7	4336.6	3801.7	1848.3	438.8	384.2
	SA-SAC	5416.0	5357.6	5205.3	5264.2	4752.7	2965.6	1149.9
	SofA-SAC* (Ours)	5744.5	5324.6	5347.4	5452.4	5004.6	2457.6	811.1
Ant $\epsilon = 0.15$	Vanilla	5379.1	645.4	767.8	472.3	162.3	83.8	86.7
	SA-SAC	6946.8	4835.9	4800.4	4487.1	2637.2	1229.3	934.6
	SofA-SAC (Ours)	6816.9	5127.3	5273.2	4990.1	3940.2	2076.4	1339.4

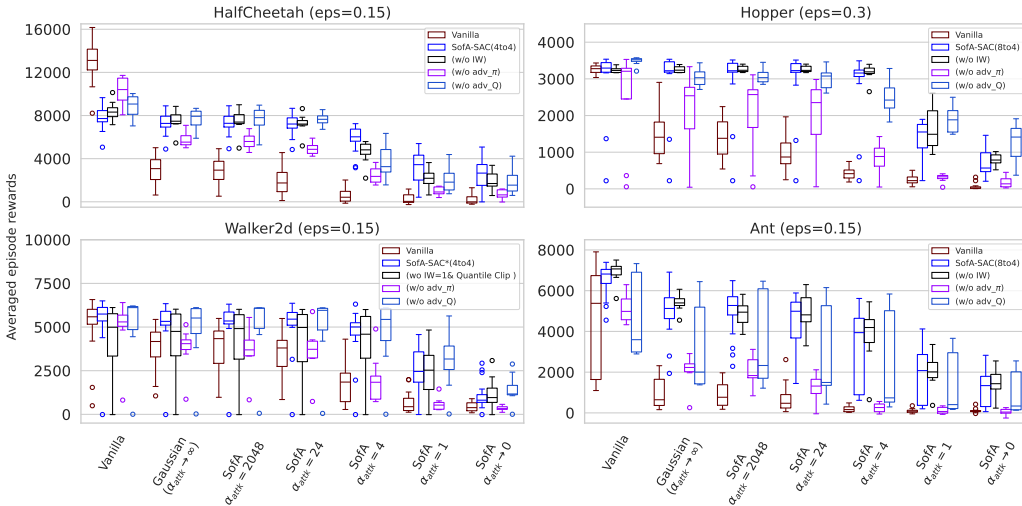


Figure 6: Ablation studies of SofA-SAC were conducted on all four tasks under Gaussian-based soft worst-case attacks. We tested versions including: neglecting the importance weight during policy improvement (w/o IW), fully omitting adversaries during policy improvement (w/o adv_π), and omitting adversaries during the updating of Q-values (w/o adv_Q).

D.2 Ablation Studies on SofA-SAC Procedures Across All Four Tasks

Fig. 6 shows the robustness evaluation results for SofA-SAC and its ablation variants. We tested three variant methods in addition to Vanilla-SAC and SofA-SAC. The first variant does not consider the importance weight in Eq. 14 during the policy improvement. The second does not involve adversaries during policy improvement, as described in Eq. 14. The last variant does not use adversaries during Q updates, as outlined in Eq. 13.

Effect of Importance Weight In HalfCheetah, the robustness of the variant that omits the importance weight is clearly inferior to that of SofA-SAC. However, in other tasks, it is competitive. We assume that the importance weight facilitates precise estimations for pessimistic scenarios under the adversary but also introduces a variance element to training.

Effect of Adversary during Policy Improvement Across all four tasks, the absence of adversaries during policy improvement results in a significant deterioration of robustness. These tendencies are particularly evident in the complex task of Ant and under strong (or large) attacks.

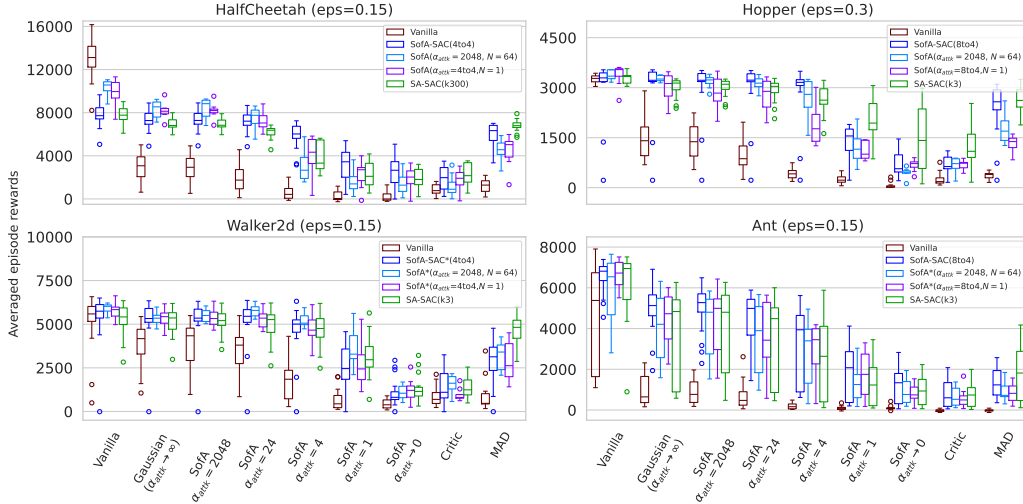


Figure 7: Ablation studies of SofA-SAC were conducted on all four tasks under Gaussian-based soft worst-case attacks. We tested versions including: one where the coefficient parameter is high (nearing randomness) with $\alpha_{attk} = 2048$, and another using only one sample to update both the policy and Q-value ($N = 1$).

Effect of Adversary during Q-update Omitting adversaries during Q-update leads to high variance and slightly inferior scores under attack evaluations. We estimate that without adversaries during Q-updates, the action values tend to be overly optimistic (under the soft worst-case scenario), which causes the policy behavior to become rough and fail to maintain good scores under perturbations.

D.3 Ablation Studies on SofA-SAC’s Sampling Settings Across All Four Tasks

To validate the differences between adding random perturbations during optimization, we examine cases where the hyperparameter is adjusted to extreme values: one variant involves increasing the temperature parameter, α_{attk} , (which approximates Gaussian perturbation), and the other uses only one sample (identical to a single sample from Gaussian perturbation). Fig. 7 displays the robustness evaluation results. SofA-SAC with $\alpha_{attk} = 4$ maintains higher scores even as attacks intensify. However, especially in the case of HalfCheetah, a clear trade-off between performance without attacks and robustness under attacked conditions is observed. The two variants outperform SofA-SAC ($\alpha_{attk} = 4$) under attack-free conditions but exhibit lower robustness under evaluation conditions with attacks.

D.4 Sensitivity Analysis of Coefficient Parameters for SofA-SAC and SA-SAC

To elucidate the characteristics of our methods and the tasks evaluated in our experiments, we present Fig. 8, which shows the average evaluation scores for SofA-SAC and SA-SAC across various coefficient trainings.

In HalfCheetah, the trade-off between performance under evaluation without attacks and robustness against attacks is evident, influenced by the coefficient parameters (α_{attk} for SofA-SAC and κ_{reg} for SA-SAC). Despite this trade-off, when comparing SofA-SAC with SA-SAC at equivalent levels of (Vanilla) evaluation, SofA-SAC appears superior for strong attacks that related to MDPs (SofA and Critic attack). In the context of the MAD attack, SA-SAC consistently achieves higher or competitive scores with strong coefficient parameters due to the integration of a consistency term into the policy’s objective function to counteract MAD attacks.

In Hopper and Walker, variants trained with weaker coefficient parameters than the main results (blue and green) maintain equivalent performance under evaluation without attacks. However, stronger attacks reveal the lack of robustness in these variants with weak coefficient parameters. Therefore, we can search for parameters that do not degrade performance without attacks but maintain a certain degree of robustness against attacks.

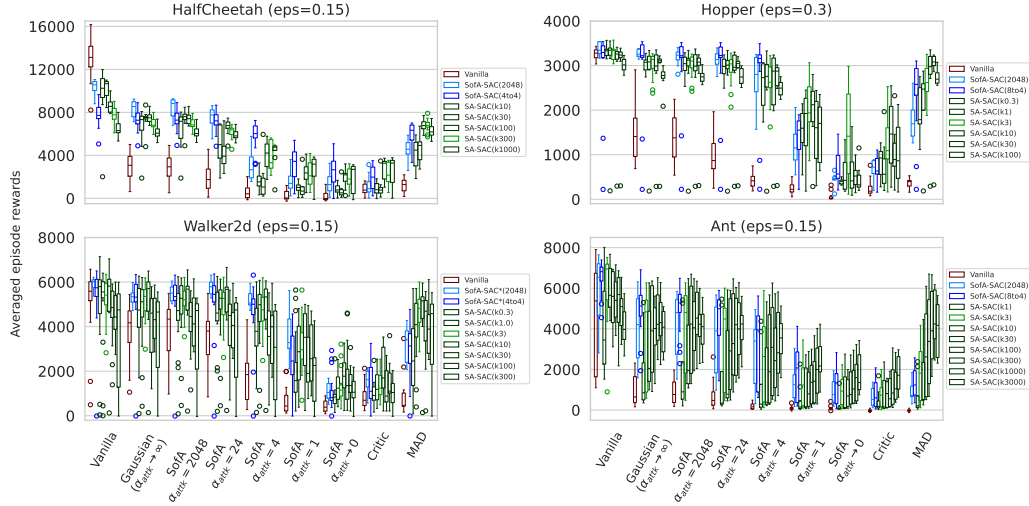


Figure 8: Box plots represent the performance of SofA-SAC and SA-SAC under Gaussian-based attacks across trainings with various coefficient parameters, including α_{atk} for SofA-SAC and κ_{reg} for SA-SAC. We use the same colors for the main settings: Vanilla (brown), SofA-SAC (blue), and SA-SAC (green). Variants of SofA-SAC and SA-SAC with different parameters are represented by light blue (for $\alpha_{atk} = 2048$) and dark green, respectively.

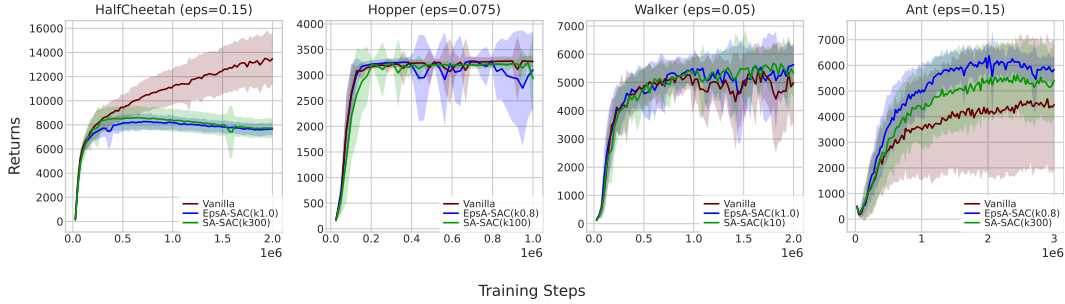


Figure 9: Learning curves for EpsA-SAC and baseline algorithms on four MuJoCo control tasks. The solid lines represent the average evaluation scores, and the shaded areas indicate the standard deviation.

In Ant, weaker coefficient parameters yield slightly inferior evaluation scores, and overly strong attacks significantly reduce natural scores. We hypothesize that due to Ant’s high-dimensional state space, a moderate level of pessimism or regularization aids in stabilizing learning. However, when regularization is excessively strong, it leads to a drop in performance without attacks due to the trade-off between the original task objective and the regularization objectives.

E Additional Results and Experiments for EpsA-SAC

In this section, we present the results of additional experiments to detail the characteristics of EpsA-SAC and validate the observed tendencies.

E.1 Learning Curves and Evaluation Score Tables for EpsA-SAC and Baseline Algorithms

Fig. 9 presents the learning curves for EpsA-SAC and baseline algorithms in Section 5.1.2. We would like to remind you that during training, EpsA-SAC utilized L_∞ -norm observation perturbations, the uniform distribution and the Critic attack, and SA-SAC maintained the consistency of the policy output under the L_∞ -norm. However, the actual trainings were executed without any perturbation. As the same as in Appendix D.1, we observe modest scores due to enhanced robustness in HalfCheetah,

Table 2: Median values of average episode rewards across 16 different seed models of original SAC, SA-SAC, and EpsA-SAC for four MuJoCo control tasks. Bold scores indicate the highest evaluation scores among the three methods.

Environment	Method	Natural Reward	Uniform ($k_{\text{worst}} = 0.0$)	EpsA ($k_{\text{worst}} = 0.4$)	EpsA ($k_{\text{worst}} = 0.8$)	Critic ($k_{\text{worst}} = 1.0$)	MAD	SA-RL	PA-AD
HalfCheetah $\epsilon = 0.15$	Vanilla	13110.6	4547.8	2435.2	1160.3	769.5	1283.4	-1139.7	-32.0
	SA-SAC	7769.3	7404.3	5240.2	3054.9	2158.0	6794.7	1064.9	1784.7
	EpsA-SAC (Ours)	7681.9	7572.8	6701.5	5495.0	4279.4	7000.7	5501.4	5327.9
Hopper $\epsilon = 0.075$	Vanilla	3278.2	3290.5	3239.9	3237.9	3236.8	3225.1	1840.1	2956.6
	SA-SAC	3191.4	3195.7	3160.0	3145.9	3096.5	3204.9	3130.2	3141.0
	EpsA-SAC (Ours)	3310.2	3319.4	3280.0	3249.7	3187.5	3340.4	3149.3	3243.2
Walker2d $\epsilon = 0.05$	Vanilla	5587.6	5347.5	4976.6	4844.4	4388.5	4648.8	2858.9	2253.1
	SA-SAC	6056.3	6054.1	5654.4	5343.9	5169.0	6025.4	5741.4	5474.3
	EpsA-SAC (Ours)	5928.8	5904.7	5769.1	5692.1	5134.8	5717.6	5224.6	5282.8
Ant $\epsilon = 0.15$	Vanilla	5379.1	1907.7	177.0	15.8	-15.1	-19.0	168.6	-542.0
	SA-SAC	5691.6	5258.3	1593.8	710.0	839.8	3901.3	3026.8	1173.1
	EpsA-SAC (Ours)	5957.3	5610.4	3666.8	2166.4	2052.1	3269.2	2821.2	4033.7

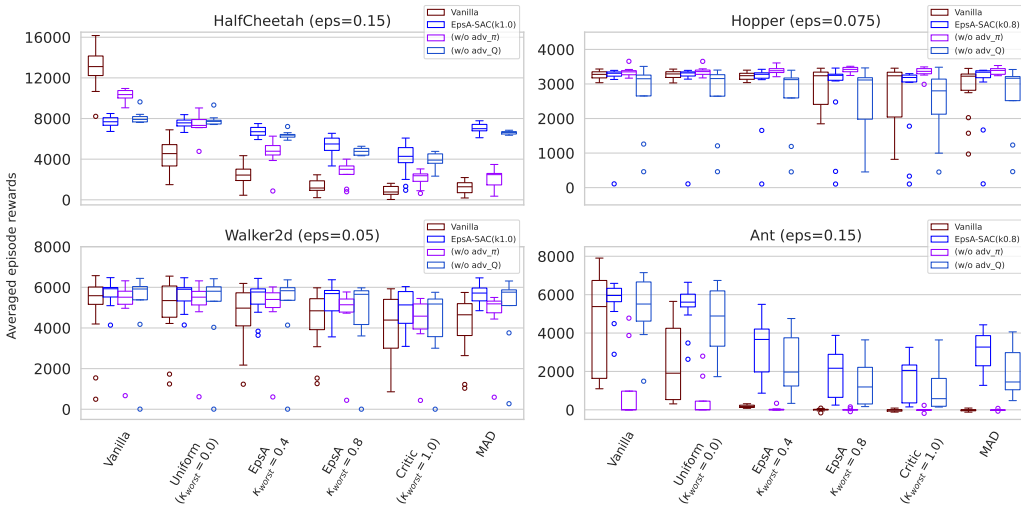


Figure 10: Ablation studies of EpsA-SAC under the L_∞ -norm based attack. We tested versions including: omitting adversaries during policy improvement (w/o adv_ π) and omitting adversaries during the updating of Q-values (w/o adv_Q).

however, we found that the introduction of EpsA-SAC and SA-SAC did not sacrifice performance. Furthermore, learnings were more stable than with Vanilla-SAC in the complex task (Ant).

E.2 Ablation Studies on EpsA-SAC Procedures Across All Four Tasks

For EpsA-SAC, we also tested the absence of adversaries during training procedures. Fig. 10 and 11 illustrate the learning curves and robust evaluation results for ablation studies that omit the adversary during policy improvement and Q-update. Although we observe tendencies similar to those in the SofA-SAC ablation study (detailed in Appendix D.2), the absence of an adversary during policy improvement typically results in reduced robustness, and its absence during Q-update leads to higher variance scores. In Hopper and Walker2d, the differences are minimal, but the collapse in Ant is severe. We assume that this is related to the observation dimension and perturbation scales that is utilized during training. As described in Appendix C.3, EpsA-SAC theoretically integrates the training framework with the assumed adversary to maintain and update a unified action-value function. However, if the attack scale increases and the observation dimensions are large, the policy can no longer produce valid actions for subsequent action values. Consequently, the target action value decreases progressively, leading to training collapse.

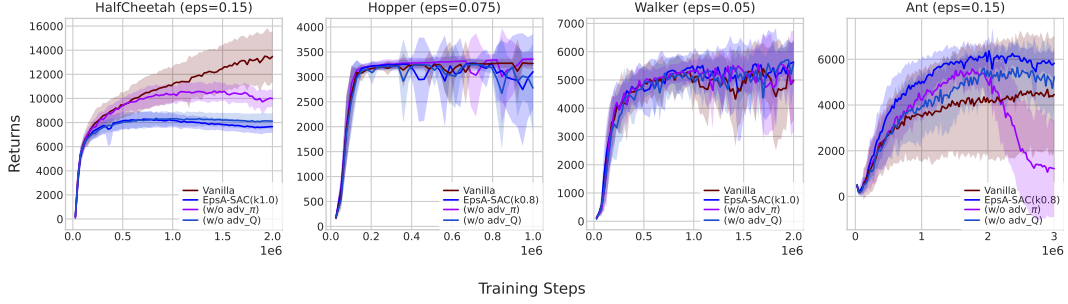


Figure 11: Learning curves of ablation studies for EpsA-SAC. We trained versions including: omitting adversaries during policy improvement (w/o adv_π) and omitting adversaries during the updating of Q-values (w/o adv_Q).

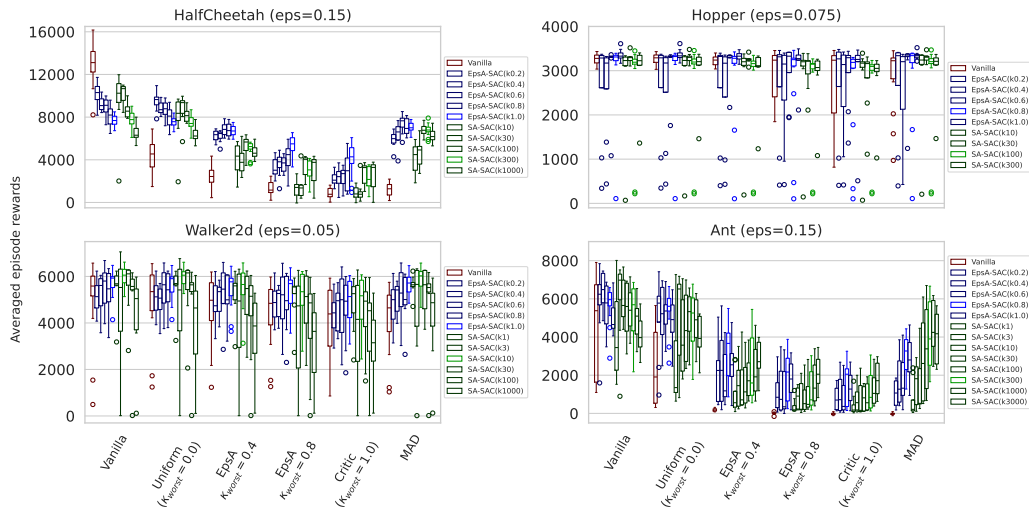


Figure 12: Box plots represent the performance of EpsA-SAC and SA-SAC under L_∞ -norm attacks across trainings with various coefficient parameters, including κ_{worst} for EpsA-SAC and κ_{reg} for SA-SAC. We use the same colors for the main settings: Vanilla (brown), EpsA-SAC (blue), and SA-SAC (green). Variants of EpsA-SAC and SA-SAC with different parameters are represented by dark blue and dark green, respectively.

E.3 Sensitivity Analysis of Coefficient Parameters for EpsA-SAC and SA-SAC

Fig. 12 displays evaluation scores from trainings with various coefficient parameters, κ_{worst} for EpsA-SAC and κ_{reg} for SA-SAC. As discussed in Appendix D.4, the trade-off between performance under attack-free evaluation and robustness is evident in HalfCheetah. In Ant, however, certain parameters optimally balance regularization, stability, robustness, and performance without attacks, demonstrating a sweet spot.

F Hyperparameter and Settings

In this section, we describe experiments settings and hyperparameter that are used in Section 5, Appendix D, and E. We use SAC [Haarnoja et al., 2018a,b] as the base algorithm. All variants, including SofA-SAC, EpsA-SAC, SA-SAC, and WocaR-SAC, generally adhere to the settings and parameters outlined in Appendix F.1, except for their specific adjustments.

Table 3: Common SAC Hyperparameter Settings

Hyperparameter	Value
Optimizer	Adam [Kingma and Ba, 2014]
Learning Rate(Actor, Critic, α_{ent})	0.0003
Discount Factor (γ)	0.99
Target Smoothing Coefficient (τ)	0.005
Optimization Interval per Steps	1
Number of Nodes	256
Number of Hidden Layers	2
Activation Function	ReLU
Prioritized Experience Replay (β_{per})	<u>start from 0.4 to 1.0 at the end</u>
Replay Buffer Size	1,000,000
Batch Size	256
Temperature Parameter (α_{ent})	Auto-tuning
Target Entropy (\mathcal{H}_{target})	$-\dim \mathcal{A} $, <u>only for Hopper-v2: $\mathcal{H}_{target} = 0.2$</u>
Normalizer	<u>state normalizer only</u>

F.1 Vanilla SAC (Common settings)

Almost all settings follow those in the second SAC paper [Haarnoja et al., 2018b]; however, it is important to note that we added procedures and modified parameters to ensure stable evaluation results across all four tasks. Specifically, we set the training steps at 1M for Hopper, 2M for HalfCheetah, 2M for Walker2d, and 3M for Ant. Table 3 lists all other settings, with underlined parts indicating the additions or modifications we made to achieve stable experimental outcomes. We explain the reasons for the modifications made, as detailed below.

Target Entropy for Hopper-v2 We found that the target entropy $\mathcal{H}_{ent} = -\dim|\mathcal{A}| = -3$, as used for Hopper-v2 in the original SAC [Haarnoja et al., 2018b], is too low to get stable final results. Consequently, scores during training oscillated drastically, a phenomenon observed not only in our SAC implementation but also in a well-known open-source implementation [Raffin et al., 2021]. Though a fixed temperature parameter $\alpha_{ent} = 0.2$, as in the first SAC paper [Haarnoja et al., 2018a], or decreasing learning rate for α_{ent} also work well, we decide to tune the target entropy only for Hopper-v2 so as to keep stable final results.

Prioritized Experience Replay We use Prioritized Experience Replay (PER) [Schaul et al., 2015] to accelerate learning outcomes. While its effect is only slightly better in some tasks, we do not observe any disadvantages to using PER. Therefore, we decide to continue to use this method.

Normalizer We normalize state inputs by recording running statistics as the agent receives information from environments. Subsequently, when the SAC agent samples a mini-batch for learning or calculating output from observation inputs, we use the state normalizer to set the mean and standard deviation to 0.0 and 1.0, respectively.

We attempt to normalize rewards by episodic returns as SA-PPO [Zhang et al., 2020] and other recent on-policy methods [Zhang et al., 2021, Oikarinen et al., 2021, Sun et al., 2021, Liang et al., 2022] did. However, we observe that the agent’s learning became critically slow in HalfCheetah due to delays in updating the running statistics. Therefore, we decided to abandon this normalizer.

F.2 SofA-SAC settings

SofA-SAC utilizes temperature parameter α_{atk} , which determines the strength of the adversary, and a sample approximation number N as its unique parameters. Typically, we set $N = 64$ during Q-update and policy improvement except for ablation studies. We find that setting α_{ent} from 4 to ∞ works well across four tasks without significantly compromising performance under attack-free evaluation, except in HalfCheetah. In Hopper and Ant, starting training with $\alpha_{atk} = 8$ and gradually decreasing it to $\alpha_{atk} = 4$ results in stable scores and enhanced robustness. This approach likely prevents pessimistic exploration during the initial training phase.

When scheduling α_{attk} , we maintain the initial value until $t = 2.5 \cdot 10^5$ steps, then linearly decrease it to reach the final target parameter at $t = \text{training-steps} - 2 \cdot 10^5$. Subsequently, we maintain this final value until the end of the training. Consequently, we denote the parameters in the legends of the graphs as '8to4' or '4to4' to clarify for the readers.

To avoid unintended unstable training in Walker2d-v2, we implement two special measures to exclude outlier values that could lead to divergence. The first measure involves percentile clipping, which restricts the next target value to the range between the 20% percentile and the 80% percentile across the perturbed next-state samples. The second measure is to disregard the importance weight during policy improvement, which, while potentially beneficial for incorporating the adversary, tends to amplify the impact of outlier values.

F.3 EpsA-SAC settings

EpsA-SAC combines uniform perturbations with an approximation of the worst attack using the mixture coefficient κ_{worst} . We employ Projected Gradient Descent (PGD) to approximate the worst attack, similarly to the approach used in the Critic attack [Pattanaik et al., 2018, Zhang et al., 2020], as detailed in Section 4.2.2. Since estimating the worst-case states that consider the entropy term of SAC is challenging, we employ two approximations: (1) using the mean of the action outputs, and (2) ignoring the entropy term. As the SAC-based algorithm’s Critic comprises two networks, we average their outputs for gradient calculations.

To balance computational resources and performance, we determine that five gradient steps with a random start during PGD suffice for our methods. To mitigate poor exploration during the initial training phase, we start $\kappa_{\text{worst}} = 0$ and linearly increase it to the target value by $t = \text{training-steps} - 2 \cdot 10^5$, maintaining this level until the end of the training.

F.4 SA-SAC settings

Originally, SA-MDP [Zhang et al., 2020] was implemented for PPO, A2C, DDPG, and DQN. We have adapted this to create a SAC version, termed SA-SAC, by appropriately extracting key elements from both SA-PPO and SA-DDPG. SA-SAC updates its policy with action consistency terms to account for cases where the attacker manipulates observations to induce actions that differ from the original ones. This loss function for policy is represented as:

$$L(\pi) = \mathbb{E}_{s \sim D(\cdot)} \left[\mathbb{E}_{a \sim \pi} [\alpha_{ent} \log \pi(a|s) - Q^\pi(s, a)] + \kappa_{reg} \max_{\tilde{s} \in \mathcal{B}_{\epsilon_p}} D_{KL}(\pi(\cdot|s) \parallel \pi(\cdot|\tilde{s})) \right], \quad (59)$$

where κ_{reg} is a coefficient term to balance the original SAC loss and consistency of actions. To solve the maximization term in Eq. (59), there are two versions for computing: one using convex relaxation and the other using Stochastic Gradient Langevin Dynamics (SGLD). We adopt SGLD due to the higher scores reported in SA-PPO [Zhang et al., 2020]. We carefully extract the essence from SA-DDPG and SA-PPO and set the configurations as follows: The attack scale increases linearly from 0 to the final target value according to a predefined schedule. This increase starts from step $t = 2.5 \cdot 10^5$ and reaches the final value at step $t = \text{training-steps} - 2 \cdot 10^5$. Additionally, we use five gradient steps in our calculations. Given the trade-off between robustness and performance under attack-free evaluation, as reported in Liang et al. [2022], we conduct a comprehensive parameter search for the coefficient term κ_{reg} among the values $\{1, 3, 10, 30, 100, 300, 1000\}$.

F.5 WocaR-SAC settings

WocaR [Liang et al., 2022] is originally implemented only for PPO, A2C, and DQN. We have adapted the essence of this method into our SAC implementation. In WocaR, the agent learns an additional action-value function and its target network, which estimate the worst-case scenario induced by the policy’s action. This action-value function for the worst-case scenario is represented as the Bellman equation associated with the Worst-Case Bellman operator \mathcal{T} as:

$$(\mathcal{T}Q)(s_t, a_t) = r(s_t, a_t) + \gamma \mathbb{E}_{s_{t+1} \sim \mathcal{F}} \left[\min_{\tilde{s}_{t+1} \in \mathcal{B}_\epsilon} Q(s_{t+1}, \mu(\tilde{s}_{t+1})) \right]. \quad (60)$$

To calculate the next worst-case action value during updates practically, they calculate action bounds using convex relaxation (IBP) [Gowal et al., 2018] and determine the worst action using PGD within

these bounds. We employ *auto_LiRPA* [Xu et al., 2020] for the convex relaxation and perform five iterations of PGD to ensure efficient computation within realistic time constraints.

During policy improvement, they enhance the gradient ascent objective of the policy by incorporating the worst-case action value, aiming to balance performance under attack-free evaluation with robustness in the worst-case attack scenario. For our SAC implementation, we implement two methods: mixing the worst action value with the analytical target value (soft-max of the Q) as:

$$L(\pi) = \mathbb{E}_{s \sim D(\cdot)} \left[\mathbb{E}_{a \sim \pi} \left[\alpha_{ent} \log \pi(a|s) - \left((1 - \kappa_{worst}) Q^\pi(s, a) + \kappa_{worst} \underline{Q}^\pi(s, a) \right) \right] \right], \quad (61)$$

combining DDPG’s policy loss with the worst action-value function by using the mean of the action, $\mu(s)$, as:

$$L(\pi_\phi) = \mathbb{E}_{s \sim D(\cdot)} \left[(1 - \kappa_{worst}) \mathbb{E}_{a \sim \pi} \left[\alpha_{ent} \log \pi(a|s) - Q^\pi(s, a) \right] - \kappa_{worst} \underline{Q}^\pi(s, \mu(s)) \right]. \quad (62)$$

To mitigate poor exploration and pessimistic learning behaviors, they schedule both the attack scale and the mixture rate of the worst-case objective throughout the policy optimization process. We initiate the attack scale at 0.0 and maintain it until $2.5 \cdot 10^5$ steps, then linearly increase it to the final scale by $t = \text{training-steps} - 2 \cdot 10^5$, maintaining this value until the end of the training. Similarly, we schedule κ_{worst} to increase from 0.0 to the final target value, testing among $\{0.2, 0.4, 0.6\}$.

Both methods in Eq. (61) and Eq. (62) learn well in smaller tasks (Pendulum, InvertedPendulum) and at the initial stages of all four tasks. However, as the attack scale increases, the performance drastically declines, leading to the collapse of training, even when we use more tighter bound method [Zhang et al., 2019] than IBP used in WocaR. We hypothesize that this is because the policy fails to learn from the worst-case scenarios due to the absence of adversaries during policy improvement. Consequently, the policy cannot produce valid actions for the next target action value, causing the worst action value to estimate increasingly poorer values as the attack scale enlarges.

A similar phenomenon is observed in the ablation experiment of EpsA-SAC in Ant-v2, which lacks an adversary during policy improvement. Therefore, our findings indicate that directly applying WocaR techniques to off-policy RL is challenging.

F.6 Evaluation settings

SAC requires more computational resources (GPUs) compared to PPO. Therefore, for evaluation, we plot the mean of 20 episodic returns, using data from sixteen different training seeds for the main result parameters (Fig. 1, Fig. 2). For other parameters and ablation studies, we conducted trainings with eight different seeds for each setting and omitted the learning type attacker evaluations (SA-RL/PA-AD). For attacker learning methods (SA-RL/PA-AD), we employ the same state normalizer learned by the agent to normalize the attacker scale. Although this approach is somewhat akin to white-box attack settings, we ensure that these settings are treated consistently, thus guaranteeing that the results are evaluated in a uniform manner.

We use box plots to represent the average evaluation scores, mitigating the variance across different training seeds. The box in each plot shows the 25%, 50% (median), and 75% percentile values, while the whiskers extend to the minimum and maximum scores within the range that is not considered outliers. Outliers are depicted as hollow circles and are defined as values beyond $1.5 \times \text{IQR}$ from the quartiles, where IQR (Interquartile Range) is the difference between the 75% and 25% percentiles.

Max Action Deifference (MAD) attack We basically follow as SA-PPO and SA-DDPG [Zhang et al., 2020]. We utilize SGLD and confirm that ten gradient iterations after random initial start are enough for the evaluations.

Critic attack We apply the modified version of Critic attack [Zhang et al., 2020], rather than the one originally proposed in Pattanaik et al. [2018]. We utilize Projected Gradient Decent (PGD) and confirm that ten gradient iterations after random initial start are enough for the evaluations. As we mentioned in Appendix F.3, SAC’s Critic comprises two networks, then we use the mean of these two action values to calculate the gradient descent.

SA-RL / PA-AD Because the network structure and the procedures (especially normalization) of SAC are quite different from PPO, we implement the SA-RL [Zhang et al., 2021] and PA-AD

Table 4: Computation times for each method

Model	Hopper	HalfCheetah	Ant
	Time (hour)		
Vanilla-SAC	7.2	16.7	23.4
SA-SAC	9.3	20.6	34.7
SofA-SAC	12.1	23.5	32.6
EpsA-SAC	17.2	35.6	53.8

[Sun et al., 2021] adversaries as the SAC agent. We use the same hyperparameter and settings as detailed in Appendix F.1, with the exception of flipping the reward term $r \rightarrow -r$ and setting the target entropy as $\mathcal{H}_{target} = -\dim|\mathcal{S}|$ only for SA-RL. We reuse the same state normalizer that was learned for the policy to simplify the process and reduce additional variance terms when learning adversaries.

Soft Worst Attack (SofA) As described in Appendix B.2 and Algorithm 1, we sample 64 perturbed states in parallel from the prior distribution (Gaussian distribution in this study). Subsequently, we calculate the probability weights for these samples. We then select one sample based on these probability weights. When we set $\alpha_{atk} \rightarrow 0$, we deterministically choose the sample that has the maximum probability weight.

Epsilon Worst Attack (EpsA) As described in Appendix C.2 and Algorithm 3, we employ the uniform distribution as the prior distribution and use the Critic attack [Pattanaik et al., 2018, Zhang et al., 2020] for approximating the worst-case attack. We utilize PGD for gradient descent and adopt ten gradient iterations, consistent with the methodology used in the Critic attack evaluation.

G Computer Resources

To clarify the time and resources required to calculate our algorithms and other baselines, we present Table 4, which shows the total training time for each algorithm. To ensure fair comparison, we use *Tesla V100 32GB* GPUs for all the trainings.

H Potential Impact

Our research primarily focuses on proposing robust RL methods and evaluation techniques, which we believe will significantly advance the practical applications of RL. However, it is important to note that robustness methods, including those proposed in our methods, require additional computational resources compared to the original RL algorithms. Consequently, utilizing these methods in scenarios where robustness is not a critical requirement may result in increased computational costs. Furthermore, as with RL in general, there exists a potential risk of misuse in applications involving automation and optimization. Nonetheless, we believe that the positive utility of assisting humanity in creating a better society far outweighs these concerns.